Doctoral Thesis

Study on the behavior of atmospheric ammonia ($NH_3(g)$) in Japan and Vietnam along with controlling factors

Nguyen Van Duy

Graduate School of Environmental Engineering

The University of Kitakyushu

February 2023

CONTENTS

LIST OF FIGURES 3

LIST OF TABLES 5

Abstract 6

Chapter 1. General introduction and methodology 9

1.1. The importance of atmospheric ammonia NH_3(g) 10

1.2. The emission sources of NH_3(g) 10

1.3. Status of NH_3(g) measurement in the world 12

1.4. The purpose of this study 13

1.5. Methodologies to determine NH_3(g) 13

1.5.1. Sampling method 13

1.5.2. Chemical analysis 16

References 19

Chapter 2. Characteristics of ambient NH_3(g) concentration in urban area of Japan (Kitakyushu and Kobe) 26

2.1. Introduction 27

2.2. Experimental 27

2.2.1. Survey site 27

2.2.2. Sampling period and seasonal classification 32

2.2.3. IC chemical analysis 32

2.2.4. Meteorological parameters 32

2.2.5. Geographic information system 33

2.3. Results and discussion 33

2.3.1. Meteorological parameters 33

2.3.2. Temporal variation 35

2.3.3. Spatial distribution 41

2.3.4. Relationship with NH_3 inventory 45

2.4. Conclusions 48

References 50

Chapter 3. Characteristics of ambient NH_3(g) concentration in downtown in Hanoi and its suburbs in Vietnam 55

3.1. Introduction 56

3.2. Experimental 57

3.2.1. Survey site 57
3.2.2. Sampling period and seasonal classification 58
3.2.3. IC Chemical analysis 59
3.2.4. Transportation of device 59
3.2.5. Meteorological parameters 60
3.3. Results and discussion 60
3.3.1. Data management for blanks 60
3.3.2. Spatial variation of concentration 64
3.3.3. Temporal variation and relationship with meteorological parameters 67
3.4. Conclusions 74
References 76
Chapter 4. Summary and future prospect 81
4.1. Summary 82
4.2. Novelty/ significance 84
4.3. Future prospect 85
Publication list 86
Acknowledgments 87
Supplementary Information 89
Appendix 97

LIST OF FIGURES

Figure 1.1. Passive sampling device schematic. 14

Figure 1.2. Passive sampling device, clip (a), and rain cap (b). 15

Figure 1.3. Pre-coated filter paper. 16

Figure 1.4. Shaker. 16

Figure 1.5. Syringe with membrane filter. 17

Figure 1.6. Ion chromatograph. 17

Figure 2.1. Location of survey sites in Kitakyushu and Kobe. 28

Figure 2.2. Temporal variations of air temperature (a) and relative humidity (b) at five selected sites in Kobe. 34

Figure 2.3. Temporal variation of absolute humidity at five selected sites in Kobe. 35

Figure 2.4. Variation of NH_3(g) concentration in one-year sampling period at survey sites in Kobe. 36

Figure 2.5. Seasonal variation of NH_3(g) concentration among the survey sites in Kobe. Difference of the NH_3(g) concentration between the seasonal mean and the annual mean: the seasonal mean – the annual mean is plotted in the vertical axis. 37

Figure 2.6. Monthly variation of NH_3(g) concentration and ambient temperature at the survey site in Kitakyushu. 39

Figure 2.7. Spatial distribution of annual mean NH_3(g) concentration in Kobe. 43

Figure 2.8. Relationship of annual mean NH_3(g) concentration with elevation of each survey site in Kobe. 44

Figure 2.9. Relationship of annual mean NH_3(g) concentration with total NH_3 emission in Kobe. 45

Figure 2.10. NH_3 emission from each emission source in NH_3 inventory in Kobe. 46

Figure 2.11. Relationships of annual mean NH_3(g) concentration with the proportion of Human&Pet (a) and Road (Exhaust) (b) to the total NH_3 emission in NH_3 inventory in Kobe. 48

Figure 3.1. Location map of sampling sites and meteorological stations in Hanoi. 57

Figure 3.2. Daily variation (a) and distribution (b) of NH_3(g) concentration at four sampling sites based on daily sampling basis in Hanoi. 65

Figure 3.3. Seasonal variation in NH_3(g) concentration of daily sampling basis in Hanoi. Dot represents the mean concentration. Whisker shows the standard deviation. Note: to avoid difficulty to see by overlapping, whiskers are drawn only at the upper side of the dots. 67

Figure 3.4. Relative humidity and temperature dependence of NH_3(g) concentration at sites B and D in Hanoi. 70

Figure 3.5. The dependence of NH_3(g) concentration on wind speed (WS) and wind direction (WD) at (a) Site A, and (b) Site C in the urban area of Hanoi. Radial data are WS [m/s]. Angular data are WD [o]. The colors denote the NH_3(g) concentrations [ppb]. 71

Figure 3.6. Relative position of survey sites with To Lich River in urban area of Hanoi. 72

Figure 3.7. Monthly variation in NH_3(g) concentration of weekly sampling basis at Site A in Hanoi. 74

LIST OF TABLES

Table 2.1. Survey sites in Kobe.....29

Table 2.2. Proportion of land use in 1 km x 1 km area around each site in Kobe. 30

Table 2.3. Annual mean NH_3(g) concentrations at each site in Kobe.....42

Table 3.1. Survey sites in Hanoi. 58

Table 3.2. Types of blank. 61

Table 3.3. Blank values of daily samples. 61

Table 3.4. Blank values of weekly samples. 63

Table 3.5. Correlation coefficients between Daily and Weekly concentration and meteorological factors. 69

Abstract

Atmospheric ammonia (NH_3(g)) plays a crucial role in atmospheric chemistry as ammonium ion (NH_4^+) derived from NH_3(g) is a significant component in the formation of secondary aerosol. However, the data set for the NH_3(g) concentration is insufficient as compared to other parameters in the air quality monitoring network (i.e., particulate matter, NO_x, SO_2) due to its measurement is not mandatory in the regulatory framework as well as the immature development of NH_3(g) auto analyzer commercially available. Agricultural emission has been determined as the major source of NH_3 inventory, however, other significant non-agricultural activities contributing to NH_3(g) emission, usually in urbanized areas, need to be thoroughly discussed. Therefore, this doctoral thesis provides detailed knowledge on the emission source, spatiotemporal characteristics and controlling factor of this gaseous pollutant in urbanized areas of both developed and developing countries (i.e., Japan and Vietnam, respectively) with the purpose of comprehensive evaluation of the behavior of this gas in the atmosphere and comparison between two countries.

The NH_3(g) concentration was measured for one year by using passive sampling method with the purpose of investigating spatiotemporal characteristics of NH_3(g) at multiple-site network. Regarding spatial distribution, the large disparity could be seen between the NH_3(g) concentration in Japan and Vietnam. In detail, in Japan, the annual mean NH_3(g) concentration was 4.28±1.7 ppb in Kitakyushu (range from 0 to 8.94 ppb), and 2.08±0.9 ppb (range from 0 ppb to around 5 ppb) in Kobe, in which, the NH_3(g) concentration at the mountainous site with high elevation was the lowest, while it was the highest at the site where the contribution of agriculture was noticeably large in the NH_3 inventory regardless of any controlling factors, followed by commercial and residential areas. When the NH_3(g) concentration in the urbanized area of Kobe is discussed, as in our present study area, the proportion of humans and pets (Human&Pet) to the total in the NH_3 inventory could be a good

parameter to account for the NH_3(g) concentration. While in Vietnam, a distinctly high concentration (79.8±61.2 ppb) was indicated at the polluted river, an important source unheard of in urban areas, followed by the crossroad (38.6±18.8 ppb) and the downtown (36.5±20.0 ppb); the lowest concentration (35.6±36.0 ppb) was observed in the rural area. The proportion of agricultural emissions in Vietnam was overwhelmed by other emission sources in urban area, suggesting that the urban area was seriously suffered from NH_3(g) pollution.

In terms of temporal variation, in both areas of Kobe and Kitakyushu, Japan, the NH_3(g) concentration indicated lower level in the summer than those in other seasons and experienced higher concentration in colder period, which was newly found compared with the conventional wisdom and results in former studies. The meteorological factors significantly contributed to the specific seasonal variation; moreover, multiple factors such as located situation, acid-base balance in the atmospheric reaction and vehicular emission were mutually related and presumably responsible for the seasonality of higher in the colder seasons and lower in the warmer season. In addition, the phenomenon of higher concentration in colder seasons was also observed in the downtown of Hanoi, Vietnam, implying the major impact of vehicular emission on the rise of NH_3(g) in urban area. However, the highest concentration in summer was observed, particularly, at polluted river and rural area due to the strong impact of temperature and relative humidity on the volatilization of NH_3(g) from wastewater and agriculture, respectively. Furthermore, the local wind was supposed to have significant impact to transfers NH_3(g) intensely emitted from a particular source to the surrounding areas, causing the homogenous characteristic (i.e., less disparity among sites) of NH_3(g) in entire area of Kobe, and the unexpectedly high concentration at the downtown in Hanoi in summer, while the transboundary transportation of air parcels seemed to have no effect on the change of NH_3(g) concentration.

The sampling transportation method used in this study may be applicable to monitor the atmospheric concentration of other gaseous species in further studies in other countries and/or distant locations thanks to the experience in conducting experiments with long-range delivery.

Keywords: Ammonia gas; Passive method; Controlling factors; Vietnam; Japan

Chapter 1. General introduction and methodology

1.1. The importance of atmospheric ammonia NH_3(g)

Ambient ammonia gas (NH_3(g)), the most abundant alkaline gas in the atmosphere (Asman, 1987), is an important contributor to various environmental pollution issues. Regarding the secondary inorganic aerosol formation in fine particulate matters ($PM_{2.5}$), ammonium salts, which are formed under the reaction of par ticulate sulfuric acid, nitric acid gas, and hydrogen chloride gas with ammonia gas, account for a large fraction of the $PM_{2.5}$ mass concentration (Gong et al., 2013; Bessagnet et al., 2014; Yamazaki et al., 2015; Backes et al., 2016; Wang et al., 2018). Regarding the nucleation of aerosols, Kulmala et al. (2002) presented a ternary nucleation (sulfuric acid–ammonia–water) model indicating the crucial role of NH_3(g) in those nucleation events. A study by McMurry et al. (2005) also revealed a positive correlation between the concentrations of nucleated particles and NH_3(g) concentration in the sulfur-rich Atlanta atmosphere. In addition, although NH_3(g) itself is an alkaline gas, NH_3(g) also distinctly affects the soil acidification and eutrophication of ecosystems through the process of nitrifying ammonium NH_4^+ (Aneja et al., 2001; Behera et al., 2013).

1.2. The emission sources of NH_3(g)

NH_3(g) emission has been determined mostly from agricultural activities (i.e., volatilization from livestock waste and the application of nitrogen fertilizers) (Sapek, 2013; Xu et al., 2017; Zhao et al., 2017); however, other significant non-agricultural activities contributing to NH_3(g) emissions, usually in urban areas, have recently drawn increased attention from researchers. Vehicle emissions (Perrino et al., 2002; Borsari et al., 2017; Suarez-Bertoa et al., 2017; Huang et al., 2018; Wang et al., 2018), industrial activities (Alebic-Juretic, 2008), and wastewater treatment plants (Reche et al., 2015; Zhang et al., 2017) could be prime instances of NH_3(g) emissions in urban regions. In which, on-road vehicular emissions have been proposed as the largest or one of the largest contributors to ammonia in urban area

(Whitehead et al., 2007; Saylor et al., 2010; Meng et al., 2011) because of the introduction of three-way catalytic (TWC) converters, selective catalytic reduction (SCR), and non-selective catalyst (NSC). The introduction of the TWC was a major step towards the vehicular emissions control, in which molecular nitrogen is the aimed reaction product during the reduction of NO_x over the TWC, however ammonia has been found to be byproduct during this process (see following reactions) (Livingston et al., 2009; Heeb et al., 2012; Yao et al., 2013).

$$CO + H_2O \rightarrow CO_2 + H_2$$

$$2NO + 2CO + 3H_2 \rightarrow 2NH_3 + 2CO_2$$

$$2NO + 5H_2 \rightarrow 2NH_3 + 2H_2O$$

$$2NO + 5CO + H_2O \rightarrow 2HNCO + 3CO_2$$

$$HNCO + H_2O \rightarrow NH_3 + CO_2$$

Besides, SCR and NSC after-treatment systems have lately been incorporated to light-duty vehicles (LDVs) as $DeNO_x$ systems, their goal is to reduce NO_x emissions by reacting the NO and NO_2 with NH_3, formed by the reduction of the urea injected into the system, on a catalyst surface; the over-doping of urea and/or the catalyst degradation may lead to ammonia emissions (Suarez-Bertoa and Astorga, 2016).

Even though studies on non-agricultural emission sources are on the rise, the fact that studies of NH_3(g) emission from these sources have still been inadequate to fully understand atmospheric environmental issues is undeniable. Even though identifying the major contributors to urban atmospheric NH_3(g) is a challenging task due to the coexistence of its many sources and sinks (Hu et al., 2014), a more comprehensive discussion about the non-agricultural emission sources existing in urban areas is essential in the scientific community.

Regarding the urban atmosphere, there are numerous different sources of NH_3(g), e.g., emissions from local traffic (Perrino et al., 2002; Li et al., 2006; Reche et al., 2012), industrial activities, waste containers; in which waste containers and other non-traffic fugitive emissions

could be important sources of NH_3(g) in the summer, whereas they are likely to be negligible in the winter due to low ambient temperature (Pandolfi et al., 2012; Reche et al., 2012). Besides, sewerage systems and humans (excreta, breath and sweat) are also contributors, in which sewage wastewater is a large uncertain source of atmospheric NH_3(g) and the emission from this source is poorly understood. Sewage lines that run below streets often have open gates on the top which can release gases (Reche et al., 2012). The NH_3(g) from agricultural areas should be taken into account to the urban area by regional transportation associated with wind direction (Walker et al., 2004; Ianniello et al., 2010).

1.3. Status of NH_3(g) measurement in the world

The NH_3(g) concentration in the ambient air has been measured by air quality monitoring networks such as the European Monitoring and Evaluation Programme (EMEP), the National Atmospheric Deposition Program (NADP) and the Acid Deposition Monitoring Network in East Asia (EANET). In some cities around the world, measurements of NH_3(g) have been reported, for example, in Rome (Perrino et al., 2002), New York State (Li et al., 2006; Zhou et al., 2019), Manchester (Whitehead et al., 2007), Barcelona (Pandolfi et al., 2012), Shanghai (Chang et al., 2016), Beijing (Ianniello et al., 2010; Zhang et al., 2018), European cities (Elser et al., 2018), Spanish cities (Reche et al., 2015), and Seoul (Phan et al., 2013).

However, the data set for the NH_3(g) concentration is insufficient as compared to other parameters which have been measured continuously in the air quality monitoring network such as sulfur dioxide, nitrogen oxides (nitrogen monoxide and nitrogen dioxide) and particulate matter. This is partially due to the immature development of NH_3(g) auto analyzers commercially available. Even though the information regarding the NH_3(g) concentration in the ambient air is insufficient, it is essential and inevitable to accumulate information on the

NH_3(g) concentration to better understand the atmospheric chemistry and the dynamics of the atmosphere.

1.4. The purpose of this study

Because of the shortage of NH_3(g) data, the primary goal of our study was to measure and build up the data set of ammonia concentration in the atmosphere of Vietnam and Japan to address this knowledge gap. Based on those data, we obtain an urban map of NH_3 concentrations for 1-year period of four seasons and then evaluate the differences of ambient ammonia concentration between Vietnam and Japan. In addition, we attempted to further identify the main sources, behavior, and controlling factors responsible for the higher concentrations of this pollutant registered in certain areas of the city. Furthermore, this research will pave a way for conducting further research relative to atmospheric environmental pollution in other cities and/or countries that require long-range delivery of samplers.

1.5. Methodologies to determine NH_3(g)

1.5.1. Sampling method

There are some methodologies for determining the NH_3(g) concentration. NH_3(g) can be collected by active method (i.e., a denuder and filter pack) and/or passive method. The denuder method has a crucial advantage in determining the NH_3(g) concentration with high accuracy thanks to no or little influence of artifacts. However, due to its complicated operation and high cost (Ferm and Hellsten, 2012), the denuder method is inappropriate for use in a network in which many survey sites must be established. The filter-pack method is also available for measuring total NH_3 concentrations. The filter-pack method is generally cheaper than the denuder method. Furthermore, the filter-pack method has an advantage in those concentrations of not only gaseous components, but also particulate matter can be concurrently

determined. On the other hand, the filter-pack method has a disadvantage of artifacts in the sampling (e.g., Matsumoto and Okita, 1998; Pathak and Chan, 2005). The passive method for determining atmospheric air quality is a method used worldwide, particularly within international frameworks such as the Acid Deposition Monitoring Network in East Asia (EANET) and the World Meteorological Organization (WMO) (Khuriganova et al., 2019). The passive sampling device is small and does not require electricity; moreover, the handling method is simple. On the other hand, the passive method also has a disadvantage of being available only for the determination of gaseous components. Taking the advantages and disadvantages of each methodology into account, the passive method is the most appropriate and effective for a campaign in which many survey sites should be established apart from each other for spatial distribution analysis, although the concentration to be determined is limited to gaseous component of ammonia $NH_3(g)$ only.

In this study, the $NH_3(g)$ concentration was determined by using Ogawa passive sampling device (OG-SN-S (filter folder) and OG-SN-17 (filter), OGAWA & CO., LTD., Kobe, Japan).

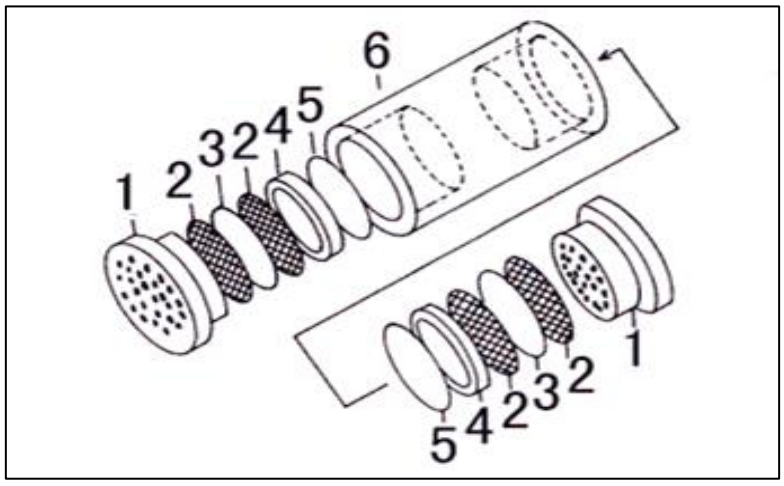

Figure 1.1. Passive sampling device schematic (Ogawausa.com).

The Ogawa Passive Sampling Device - PSD (Fig. 1.1) is a small polymer device with a cylindrical shape. It is 3 cm in length and 2 cm in diameter. It holds two collection filters, one

on each side. The collection filters are held between two stainless steel screens. The screens and filters are held in place with an endcap. The caps have 25 holes to allow ammonia to diffuse through to the filter. The PSD is placed in a plastic holder that is then placed in a rain shelter (Fig. 1.2). The rain shelters are standard 4" PVC pipe endcaps.

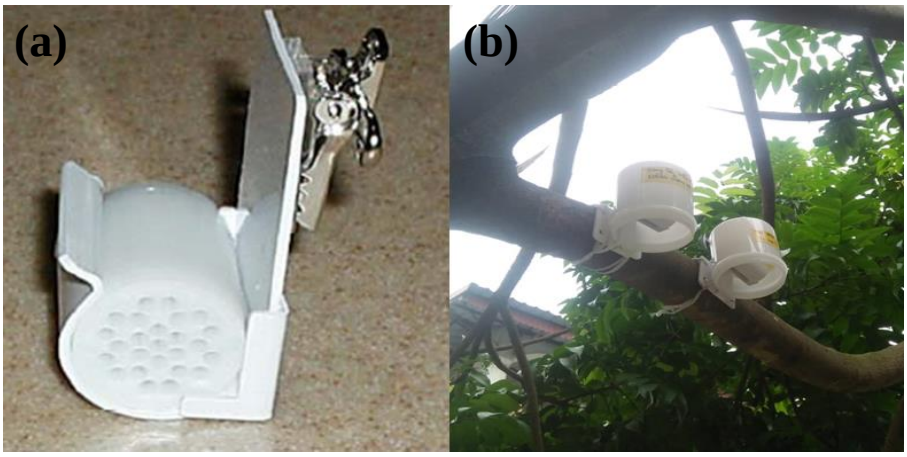

Figure 1.2. Passive sampling device, clip (a), and rain cap (b).

Principle of determination of concentration: in a passive sampler the target compound diffuses to the absorbent. The sampling rate (volume/time) is determined by the diffusion coefficient of the target analyze and the shape and design of the sampler. For this research, phosphoric acid (H_3PO_4) was used as the absorbent. The ammonia reacts with the phosphoric acid coated in the filter paper (Fig. 1.3) to form ammonium dihydrogen phosphate. This "traps" the ammonia on the filter, which is later extracted using water and analyzed using ion chromatography.

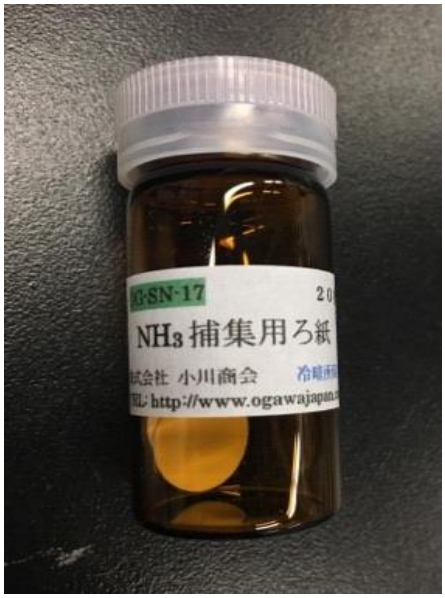

Figure 1.3. Pre-coated filter paper.

1.5.2. Chemical analysis

Preparation for Ion chromatogram analysis

The exposed filter paper was put into Iboy bottle (50 ml), and then deionized water (10 ml) was used in the extraction of the filter paper by using shaker with the speed of 200 rotations per minute in 20 minutes (Fig. 1.4).

Figure 1.4. Shaker.

A small amount of extraction solution, then, was filtered into the IC vial using syringe attached to membrane filter of 0.45 μm in diameter (Fig. 1.5). The syringe and membrane filter were washed carefully with ultrapure water and drained by a small amount of extraction solution again before filtering. These steps were repeated after each time of filtering sample.

Figure 1.5. Syringe with membrane filter.

Ion Chromatography analysis

The extracts were measured with an Ion chromatograph (Fig. 1.6) for ammonium NH_4^+ analysis as soon as possible after collection.

Figure 1.6. Ion chromatograph.

Conversion method to atmospheric ammonia concentration

From the analyzed results of Ion chromatograph, the atmospheric ammonia concentration was calculated based on the following equation:

$$C(NH_3) = \frac{m(NH_4^+) \times v \times \alpha}{t}$$

In which:

$C(NH_3)$: The concentration of sampled gas (ppb)

$m(NH_4^+)$: The concentration of NH_4^+ determined in the extract solution (ng/ml)

v: The extraction volume of the filter (ml)

α: NH_3 atmospheric concentration conversion factor

α=87.6 x (293 / (273 + T))$^{1.83}$ (T: atmospheric temperature)

87.6 ppb.min.ng-1 (in case of extract 1 filter paper)

43.8 ppb.min.ng-1 (in case of extract 2 filter papers) (20℃, 70 %)

t : The time of exposure (min)

References

Alebic-Juretic, A. (2008). Airborne ammonia and ammonium within the Northern Adriatic area, Croatia. *Environmental Pollution* **154**: 439–447. https://doi.org/10.1016/j.envpol.2007.11.029.

Aneja, V.P., Bunton, B., Walker, J.T., Malik, B.P. (2001). Measurement and analysis of atmospheric ammonia emissions from anaerobic lagoons. *Atmospheric Environment* **35**: 1949–1958. https://doi.org/10.1016/S1352-2310(00)00547-1.

Asman, W.A.H. (1987). Atmospheric Behaviour of Ammonia and Ammonium.

Backes, A. M., Aulinger, A., Bieser, J., Matthias, V. and Quante, M. (2016). Ammonia emissions in Europe, part II: How ammonia emission abatement strategies affect secondary aerosols. *Atmospheric Environment* **126**: 153–161. https://doi.org/10.1016/j.atmosenv.2015.11.039.

Behera, S.N., Sharma, M., Aneja, V.P., Balasubramanian, R. (2013). Ammonia in the atmosphere: A review on emission sources, atmospheric chemistry and deposition on terrestrial bodies. *Environmental Science and Pollution Research* **20**: 8092–8131. https://doi.org/10.1007/s11356-013-2051-9.

Bessagnet, B., Beauchamp, M., Guerreiro, C., de Leeuw, F., Tsyro, S., Colette, A., Meleux, F., Rouil, L., Ruyssenaars, P., Sauter, F., Velders, G. J. M., Foltescu, V. L. and van Aardenne, J. (2014). Can further mitigation of ammonia emissions reduce exceedances of particulate matter air quality standards? *Environmental Science & Policy* **44**: 149–163. https://doi.org/10.1016/j.envsci.2014.07.011.

Borsari, V., Assunção, J.V. de (2017). Ammonia emissions from a light-duty vehicle. *Transportation Research Part D: Transport and Environment* **51**: 53–61. https://doi.org/10.1016/j.trd.2016.12.008.

Chang, Y., Zou, Z., Deng, C., Huang, K., Collett, J. L., Lin, J., Zhuang, G. (2016). The importance of vehicle emissions as a source of atmospheric ammonia in the megacity of Shanghai. *Atmospheric Chemistry and Physics* **16(5)**: 3577–3594. https://doi.org/10.5194/acp-16-3577-2016.

Elser, M., El-Haddad, I., Maasikmets, M., Bozzetti, C., Wolf, R., Ciarelli, G., Slowik, J.G., Richter, R., Teinemaa, E., Hüglin, C., Baltensperger, U., Prévôt, A.S.H. (2018). High contributions of vehicular emissions to ammonia in three European cities derived from mobile measurements. *Atmospheric Environment* **175**: 210–220. https://doi.org/10.1016/j.atmosenv.2017.11.030.

Ferm, M., Hellsten, S., 2012. Trends in atmospheric ammonia and particulate ammonium concentrations in Sweden and its causes. *Atmospheric Environment* **61:** 30–39. https://doi.org/10.1016/j.atmosenv.2012.07.010.

Gong, L., Lewicki, R., Griffin, R. J., Tittel, F. K., Lonsdale, C. R., Stevens, R. G., Pierce, J. R., Malloy, Q. G. J., Travis, S. A., Bobmanuel, L. M., Lefer, B. L. and Flynn, J. H. (2013). Role of atmospheric ammonia in particulate matter formation in Houston during summertime. *Atmospheric Environment* **77**: 893–900. https://doi.org/10.1016/j.atmosenv.2013.04.079.

Heeb, N. V., Haag, R., Seiler, C., Schmid, P., Zennegg, M., Wichser, A., Ulrich, A., Honegger, P., Zeyer, K., Emmenegger, L., Zimmerli, Y., Czerwinski, J., Kasper, M., Mayer, A. (2012). Effects of a combined diesel particle filter-DeNO_x system (DPN) on reactive nitrogen compounds emissions: A parameter study. *Environmental Science and Technology* **46**: 13317-13325. https://doi.org/10.1021/es3029389.

Hu, Q., Zhang, L., Evans, G. J., Yao, X. (2014). Variability of atmospheric ammonia related to potential emission sources in downtown Toronto, Canada. *Atmospheric Environment* **99**: 365-373. https://doi.org/10.1016/j.atmosenv.2014.10.006.

Huang, C., Hu, Q., Lou, S., Tian, J., Wang, R., Xu, C., An, J., Ren, H., Ma, D., Quan, Y., Zhang, Y., Li, L. (2018). Ammonia Emission Measurements for Light-Duty Gasoline Vehicles in China and Implications for Emission Modeling. *Environmental Science and Technology* **52**: 11223–11231. https://doi.org/10.1021/acs.est.8b03984.

Ianniello, A., Spataro, F., Esposito, G., Allegrini, I., Rantica, E., Ancora, M.P., Hu, M., Zhu, T. (2010). Occurrence of gas phase ammonia in the area of Beijing (China). *Atmospheric Chemistry and Physics* **10**: 9487–9503. https://doi.org/10.5194/acp-10-9487-2010.

Khuriganova, O.I., Obolkin, V.A., Golobokova, L.P., Bukin, Y.S., Khodzher, T. V. (2019). Passive sampling as a low-cost method for monitoring air pollutants in the Baikal Region (Eastern Siberia). *Atmosphere, 10*(8). https://doi.org/10.3390/atmos10080470.

Kulmala, M., Korhonen, P., Napari, I., Karlsson, A., Berresheim, H., O'Dowd, C.D. (2002). Aerosol formation during PARFORCE: Ternary nucleation of H_2SO_4, NH_3, and H_2O. *Journal of Geophysical Research* **107**: (D19) 8111. https://doi.org/10.1029/2001JD000900.

Li, Y., Schwab, J. J. and Demerjian, K. L. (2006). Measurements of ambient ammonia using a tunable diode laser absorption spectrometer: Characteristics of ambient ammonia emissions in an urban area of New York City. *Journal of Geophysical Research: Atmospheres* **111(D10)**: n/a-n/a. https://doi.org/10.1029/2005JD006275.

Li, Y., Schwab, J. J. and Demerjian, K. L. (2006). Measurements of ambient ammonia using a tunable diode laser absorption spectrometer: Characteristics of ambient ammonia emissions in an urban area of New York City. *Journal of Geophysical Research: Atmospheres* **111(D10)**: n/a-n/a. https://doi.org/10.1029/2005JD006275.

Livingston, C., Rieger, P., Winer, A. (2009). Ammonia emissions from a representative in-use fleet of light and medium-duty vehicles in the California South Coast Air Basin.

Atmospheric Environment **43**: 3326–3333. https://doi.org/10.1016/j.atmosenv.2009.04.009.

Matsumoto, M., Okita, T. (1998). Long term measurements of atmospheric gaseous and aerosol species using an annular denuder system in Nara, Japan. *Atmospheric Environment* **32**: 1419–1425. https://doi.org/10.1016/S1352-2310(97)00270-7.

McMurry, P.H., Fink, M., Sakurai, H., Stolzenburg, M.R., Mauldin, I.L., Smith, J., Eisele, F., Moore, K., Sjostedt, S., Tanner, D., Huey, L.G., Nowak, J.B., Edgerton, E., Voisin, D. (2005). A criterion for new particle formation in the sulfur-rich Atlanta atmosphere. *Journal of Geophysical Research* **110**: 1–10. https://doi.org/10.1029/2005JD005901.

Meng, Z. Y., Lin, W. L., Jiang, X. M., Yan, P., Wang, Y., Zhang, Y. M., Jia, X. F., Yu, X. L. (2011). Characteristics of atmospheric ammonia over Beijing, China. *Atmospheric Chemistry and Physics* **11(12)**: 6139-6151. https://doi.org/10.5194/acp-11-6139-2011.

Pandolfi, M., Amato, F., Reche, C., Alastuey, A., Otjes, R. P., Blom, M. J. and Querol, X. (2012). Summer ammonia measurements in a densely populated Mediterranean city. *Atmospheric Chemistry and Physics* **12(16)**: 7557–7575. https://doi.org/10.5194/acp-12-7557-2012.

Pathak, R.K., Chan, C.K. (2005). Inter-particle and gas-particle interactions in sampling artifacts of $PM_{2.5}$ in filter-based samplers. *Atmospheric Environment* **39**: 1597–1607. https://doi.org/10.1016/j.atmosenv.2004.10.018.

Perrino, C., Catrambone, M., Di Menno Di Bucchianico, A. and Allegrini, I. (2002). Gaseous ammonia in the urban area of Rome, Italy and its relationship with traffic emissions. *Atmospheric Environment* **36(34)**: 5385–5394. https://doi.org/10.1016/S1352-2310(02)00469-7.

Phan, N.-T., Kim, K.-H., Shon, Z.-H., Jeon, E.-C., Jung, K., Kim, N.-J., 2013. Analysis of ammonia variation in the urban atmosphere. *Atmospheric Environment* **65:** 177–185. https://doi.org/10.1016/j.atmosenv.2012.10.049.

Reche, C., Viana, M., Karanasiou, A., Cusack, M., Alastuey, A., Artiñano, B., Revuelta, M. A., López-Mahía, P., Blanco-Heras, G., Rodríguez, S., Sánchez de la Campa, A., Fernández-Camacho, R., González-Castanedo, Y., Mantilla, E., Tang, Y. S. and Querol, X. (2015). Urban NH_3 levels and sources in six major Spanish cities. *Chemosphere* **119**: 769–777. https://doi.org/10.1016/j.chemosphere.2014.07.097.

Reche, C., Viana, M., Pandolfi, M., Alastuey, A., Moreno, T., Amato, F., Amato, F., Ripoll, A. and Querol, X. (2012). Urban NH_3 levels and sources in a Mediterranean environment. *Atmospheric Environment* **57**: 153–164. https://doi.org/10.1016/j.atmosenv.2012.04.021.

Sapek, A. (2013). Ammonia emissions from non-agricultural sources. *Polish Journal of Environmental Studies* **22(1)**: 63–70. http://www.pjoes.com/Ammonia-Emissions-from-Non-Agricultural-r-nSources,88952,0,2.html (last access: 2021/10/29).

Saylor, R.D., Edgerton, E.S., Hartsell, B.E., Baumann, K., Hansen, D.A., 2010. Continuous gaseous and total ammonia measurements from the southeastern aerosol research and characterization (SEARCH) study. *Atmospheric Environment* **44:** 4994–5004. https://doi.org/10.1016/J.ATMOSENV.2010.07.055.

Suarez-Bertoa, R., Astorga, C., 2016. Isocyanic acid and ammonia in vehicle emissions. *Transportation Research Part D: Transport and Environment* **49:** 259–270. https://doi.org/10.1016/j.trd.2016.08.039.

Suarez-Bertoa, R., Mendoza-Villafuerte, P., Riccobono, F., Vojtisek, M., Pechout, M., Perujo, A., Astorga, C. (2017). On-road measurement of NH_3 emissions from gasoline and diesel passenger cars during real world driving conditions. *Atmospheric Environment* **166**: 488–497. https://doi.org/10.1016/j.atmosenv.2017.07.056.

Walker, J. T., Whitall, D. R., Robarge, W. and Paerl, H. W. (2004). Ambient ammonia and ammonium aerosol across a region of variable ammonia emission density. *Atmospheric Environment* **38(9)**: 1235–1246. https://doi.org/10.1016/j.atmosenv.2003.11.027.

Wang, C., Yin, S., Bai, L., Zhang, X., Gu, X., Zhang, H., Lu, Q and Zhang, R. (2018). High-resolution ammonia emission inventories with comprehensive analysis and evaluation in Henan, China, 2006–2016. *Atmospheric Environment* **193**: 11–23. https://doi.org/10.1016/j.atmosenv.2018.08.063.

Wang, R., Ye, X., Liu, Y., Li, H., Yang, X., Chen, J., Gao, W. and Yin, Z. (2018). Characteristics of atmospheric ammonia and its relationship with vehicle emissions in a megacity in China. *Atmospheric Environment* **182**: 97–104. https://doi.org/10.1016/j.atmosenv.2018.03.047.

Whitehead, J.D., Longley, I.D., Gallagher, M.W. (2007). Seasonal and diurnal variation in atmospheric ammonia in an urban environment measured using a quantum cascade laser absorption spectrometer. *Water, Air and Soil Pollution* **183**: 317-329. https://doi.org/10.1007/s11270-007-9381-5.

Xu, P., Koloutsou-Vakakis, S., Rood, M.J., Luan, S. (2017). Projections of NH_3 emissions from manure generated by livestock production in China to 2030 under six mitigation scenarios. *Science of the Total Environment* **607**: 78–86. https://doi.org/10.1016/j.scitotenv.2017.06.258.

Yamazaki, T., Takahashi A. and Matsuda K. (2015). Difference of dry deposition between sulfate and nitrate in PM2.5 to a forest in suburban Tokyo by vertical profile observations. *Journal of Japan Society for Atmospheric Environment* **50(4)**: 167-175 (In Japanese with English Abstract). https://doi.org/10.11298/taiki.50.167.

Yao, X., Hu, Q., Zhang, L., Evans, G.J., Godri, K.J., Ng, A.C. (2013). Is vehicular emission a significant contributor to ammonia in the urban atmosphere? *Atmospheric Environment* **80**: 499–506. https://doi.org/10.1016/j.atmosenv.2013.08.028.

Zhang, C.L., Geng, X.S., Wang, H., Zhou, L., Wang, B.G. (2017). Emission factor for atmospheric ammonia from a typical municipal wastewater treatment plant in South China. *Environmental Pollution* **220**: 963–970. https://doi.org/10.1016/j.envpol.2016.10.082.

Zhang, Y., Tang, A., Wang, D., Wang, Q., Benedict, K., Zhang, L., Liu, D., Li, Y., Collett Jr., J.L., Sun, Y., Liu, X. (2018). The vertical variability of ammonia in urban Beijing, China. *Atmospheric Chemistry and Physics* **18**: 16385–16398. https://doi.org/10.5194/acp-18-16385-2018.

Zhao, Z.Q., Bai, Z.H., Winiwarter, W., Kiesewetter, G., Heyes, C., Ma, L. (2017). Mitigating ammonia emission from agriculture reduces $PM_{2.5}$ pollution in the Hai River Basin in China. *Science of the Total Environment* **609**: 1152–1160. https://doi.org/10.1016/j.scitotenv.2017.07.240.

Zhou, C., Zhou, H., Holsen, T. M., Hopke, P. K., Edgerton, E. S., Schwab, J. J. (2019). Ambient Ammonia Concentrations Across New York State. *Journal of Geophysical Research: Atmospheres* **124(14)**: 8287-8302. https://doi.org/10.1029/2019JD030380.

Chapter 2. Characteristics of ambient NH_3(g) concentration in urban area of Japan (Kitakyushu and Kobe)

2.1. **Introduction**

The Japan Environmental Laboratories Association (JELA) has been measuring the NH_3(g) concentration at more than 20 sites since 1991. The JELA has clarified the NH_3(g) concentration level mainly in the urban areas of Japan and published fruitful bulletin reports (e.g., the Japan Environmental Laboratories Association, 2017).

Furthermore, Aikawa et al. (2008) studied in detail not only the characteristic variation of the concentration but also the chemical form of NH_3(g) and particulate ammonium NH_4^+ at several sites in urban and rural area of Japan. However, we must admit that studies of the NH_3(g) concentration have still been inadequate.

For this chapter, we surveyed the NH_3(g) concentration at various sites in Kobe and Kitakyushu cities with the presence of both urbanized, industrial, agricultural, and mountainous area. This study investigated the spatial and temporal distribution of the NH_3(g) concentration along with the analysis of some considered parameters as suspected controlling factors with the purposes of characterizing new behavior of NH_3(g) in the atmosphere and finding out how related impact factors accounting for the NH_3(g) concentration.

2.2. **Experimental**

2.2.1. **Survey site**

Figure 2.1 shows the location of survey sites in both Kobe and Kitakyushu area. There were nine sampling sites within a 20-km x 20-km region in Kobe City, Japan. The sampling in Kobe was conducted by Aikawa et al.. Kobe City, with a population density of more than 1,480,000 people/550 km^2, is one of the most urbanized cities in Japan. Its southern shorelines are on the Pacific Ocean through the Seto Inland Sea. Rokko mountain (Mt. Rokko), with a summit of 962 meters above sea level (a.s.l.), is in Kobe City. Mt. Rokko is subject to air pollutants transported from a highly industrialized downtown area located on the southern face of Mt. Rokko.

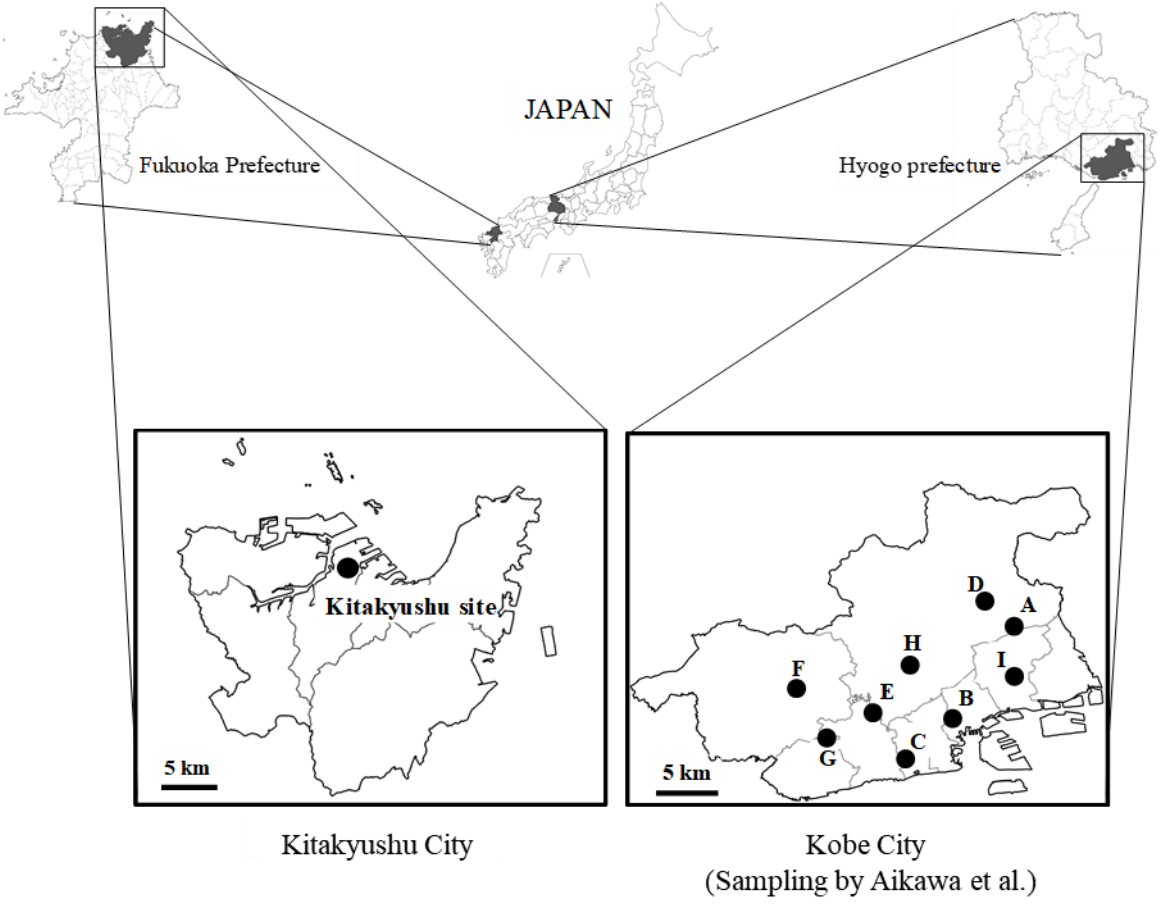

Figure 2.1. Location of survey sites in Kitakyushu and Kobe.

The characteristics of each site are summarized in Table 2.1.

Table 2.1. Survey sites in Kobe.

Sites	Latitude	Longitude	Elevation /m	Zone restrictions
Site A	34°45'27.7"N	135°13'46.2"E	800	Forest in National Park
Site B	34°41'00.6"N	135°10'12.0"E	25	Commercial, Residential
Site C	34°38'58.6"N	135°07'55.2"E	5	Light-industrial, Residential
Site D	34°46'50.9"N	135°12'08.3"E	370	Residential
Site E	34°41'16.8"N	135°06'08.6"E	180	Residential
Site F	34°42'16.6"N	135°01'59.2"E	85	Residential
Site G	34°39'59.8"N	135°03'40.0"E	105	Residential
Site H	34°43'44.4"N	135°08'09.2"E	335	Residential
Site I	34°42'57.2"N	135°13'49.1"E	55	Residential, Commercial

Besides, in order to analyze the spatial distribution of NH_3(g) in Kobe, the proportion of land use around nine survey sites in Kobe are summarized in Table 2.2, using the land use data prepared by the National Land Agency of Japan. Approximately 1-km x 1-km mesh data including the survey sites were used in analyses. The sites in Kobe are described as follows:

Table 2.2. Proportion of land use in 1 km x 1 km area around each site in Kobe.

	Paddy field & Agriculture	Forest	Building	Traffic	River & Sea	Other
Site A	0.00	**<u>0.83</u>**	**0.14**	0.02	0.00	0.01
Site B	0.00	0.00	**<u>0.84</u>**	0.07	0.00	**0.09**
Site C	0.00	0.00	**<u>0.74</u>**	**0.20**	0.00	0.06
Site D	0.16	**0.24**	**<u>0.44</u>**	0.04	0.01	0.11
Site E	0.01	0.08	**<u>0.67</u>**	**0.12**	0.00	0.12
Site F	**0.10**	**<u>0.68</u>**	0.06	**0.10**	0.02	0.04
Site G	0.05	0.21	**<u>0.50</u>**	0.01	0.01	**0.22**
Site H	0.03	**0.30**	**<u>0.56</u>**	0.00	0.00	0.11
Site I	0.00	0.00	**<u>0.86</u>**	**0.13**	0.00	0.01

Note: Bold and underline figures show the largest proportion at each site.

Bold figures show the second largest proportion at each site.

Site A: Site A was established near the top of Mt. Rokko. The altitude of the site is 800 meters a.s.l. There is one road in the vicinity (about 40 meters) of Site A, although the traffic is less than 1,000 vehicles per day. Based on the proportion of land use, forest occupies up to 83 percent of the total area, followed by building section with 14 percent.

Sites B and I: Sites B and I were established near the downtown of Kobe City. Many facilities, such as a marketplace, library and hospital, are located near Sites B and I. Both a residential district and a commercial district are nearby. In these kinds of area, the building section accounts for around 85 percent of the total land use, followed by traffic section with 7 percent in Site B and 13 percent in Site I.

Site C: Site C was established in the vicinity of the open coast. Site C is about 500 meters from the Seto Inland Sea. A residential area, as well as an industrial district, surrounds

Site C; the building section takes 74 percent of the total land use. There are two busy roads in the immediate vicinity (within about 100 meters) of Site C: a national road (around 48,000 vehicles/day) and a highway (nearly 100,000 vehicles/day), which causes the traffic in this area reaching 20 percent of the total land use.

Sites D and H: Sites D and H were established in the northern part of Kobe City, on the north side of Mt. Rokko. The area where Sites D and H were established is designated as a residential district; on the other hand, a forest area remains and is responsible for 24 and 30 percent, respectively. The concentration of air pollutants on the north side of Mt. Rokko is generally lower than that on the south side because many commercial facilities and roads with heavy traffic are concentrated on the south side of Mt. Rokko.

Sites E, F and G: Sites E, F and G were established in the western part of Kobe City. The areas around Sites E, F and G have been developed and designated as residential areas with 67 percent and 50 percent of building section in Site E and G, respectively. However, lots of forest and agricultural fields still remain around Site F because it was established in the westernmost part of Kobe City, in which there is 68 percent of forest and 10 percent of paddy field and agriculture, while only 6 percent of building section exists here.

Kitakyushu City is a well-known urbanized and industrial area in Japan since 19th century, which mainly focus on heavy industries such as steel manufacturing and chemical industry. The sampling site in Kitakyushu was established in Tobata ward, which is the most typical representative of urbanized area in Kitakyushu City with the typical presence of the Nippon Steel company nearby.

Sites A, D, E, F, G, H and I: The sampler was installed at a height of 1.5 meters above the ground.

Sites B and C: The sampler was installed at a height of 1 meter above the rooftop (rooftop: about 25 meters above the ground) of the Public Health Science Research Center of

Hyogo Prefecture (Site B) and the Hyogo Prefectural Institute of Environmental Sciences (Site C).

At the site of Kitakyushu, the sampler was installed at a height of 15 meters above the ground.

2.2.2. **Sampling period and seasonal classification**

The samples were collected on a bi-weekly basis from September 2008 to August 2009 in Kobe, and weekly basis from March 2018 to February 2019 in Kitakyushu.

There are four typical seasons in Japan, i.e., spring (March, April and May), summer (June, July and August), autumn (September, October and November) and winter (December, January and February). The seasonal classification was used in seasonal analyses: spring (March-May), summer (June-August), autumn (September-November) and winter (December-February).

2.2.3. **IC chemical analysis**

The ion chromatograph system; DX-300 series (Dionex Corp., Sunnyvale, USA) includes a pre-column, a separation column and an auto-suppressor was used for Kobe samples, and Thermo Scientific™ Dionex™ Integrion (Thermo Fisher Scientific Inc., Massachusetts, USA) was used for Kitakyushu samples.

2.2.4. **Meteorological parameters**

In the passive method, the meteorological parameters of air temperature and relative humidity are essential to calculate the concentration. The Meteorological Agency of Japan measures the parameters at only one site in Kobe City: the Kobe Marine Observatory. In this study, we aim to determine the NH_3(g) concentration in a relatively narrow region (20 km x 20

km). Furthermore, the elevations of the survey sites were quite different (Table 2.1). The only data set observed in the Kobe Marine Observatory would be insufficient for our present study. Therefore, we measured the meteorological parameters at 5 selected sites (Sites A, B, C, D and E) among the 9 sites in Kobe described above (Section 2.1.1). The air temperature and relative humidity were measured hourly using a thermometer (TR-72U, T&D Corp., Nagano, Japan). The air temperature was calibrated with a thermostat. The thermometer was installed in a simple, naturally ventilated wooden thermometer shelter (Site C) and in a solar radiation shield (CO-RS1, CLIMATEC Inc., Tokyo, Japan) (Sites A, B, D and E) positioned at the same height of the passive sampler.

At Kitakyushu site, the meteorological parameters of air temperature and relative humidity have been obtained hourly basis only at the Kitakyushu Observation Station nearby the sampling site.

The data of wind speed observed by Kobe City government around Sites A and C (Kobe City, 2008; 2009) was adapted in the discussions of Section 2.2.2 and 2.2.3.

2.2.5. **Geographic information system**

A geographic information system (ArcView) (Esri Japan Corporation, Tokyo, Japan) was used for the spatial analysis of the $NH_3(g)$ concentration in Kobe. An inverse distance-weighted method was employed to determine the distribution of the $NH_3(g)$ concentration.

2.3.**Results and discussion**

2.3.1. **Meteorological parameters**

Figures 2.2(a) and (b) show the temporal variations of air temperature and relative humidity at five selected sites in Kobe, respectively. The air temperature at Site A was the lowest, followed by Site D < Site E ~ Site B ~ Site C. The order of the air temperature was

mostly determined by the elevation. The relative humidity at Site A was the highest, followed by Site D > Site B > Site E > Site C.

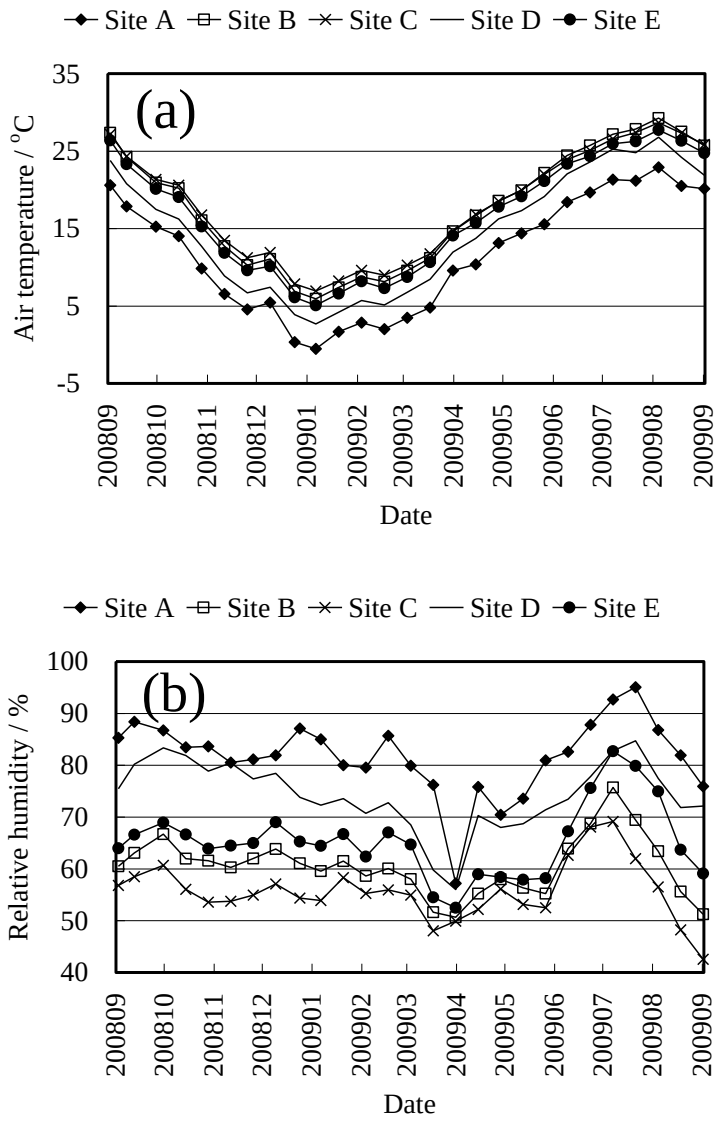

Figure 2.2. Temporal variations of air temperature (a) and relative humidity (b) at five selected sites in Kobe.

Figure 2.3 shows the temporal variation of the absolute humidity. The absolute humidity was almost the same among all sites during entire sampling period except for the summer, indicating that the relative humidity is determined via the air temperature and the absolute humidity except in the summer. We could not identify reasons for the lower absolute humidity at Sites A and C in the summer. Since large variations among the sites were observed

in not only air temperature but also relative humidity, it is inappropriate to apply the only data measured at the Kobe Marine Observatory for all sites in Kobe.

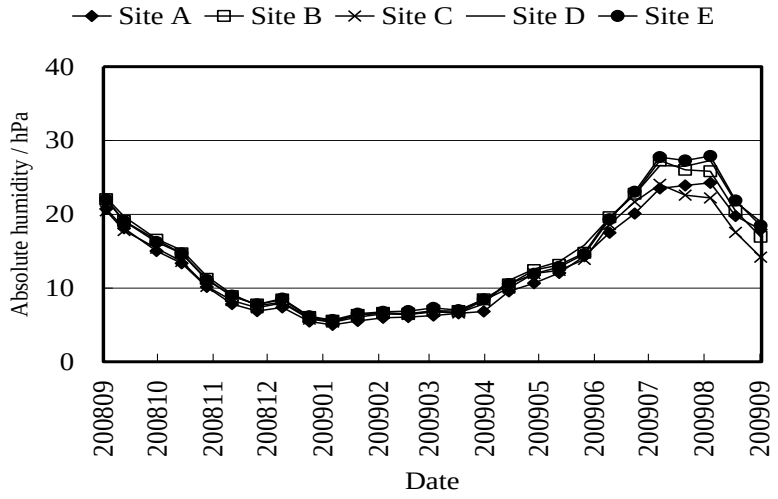

Figure 2.3. Temporal variation of absolute humidity at five selected sites in Kobe.

Using the meteorological data measured at the 5 selected sites could be more accurate in the present study. Here, the meteorological data at Site E was applied to Sites F and G, and those at Sites B and D were applied to Sites I and H, respectively. This group application was decided based on the vicinity of each site with each other, the similarity in terms of the elevation of setting samplers and the proportion of land use so that each group of sites tends to have the most typical characteristics.

In Kitakyushu, because there is one sampling site, the data collected from the Kitakyushu Observation Station was adapted directly to the following analysis of temporal variation of the NH_3(g) concentration in Kitakyushu (see Section 2.2.2).

2.3.2. **Temporal variation**

Figure 2.4 shows the variation of the NH_3(g) concentration over the course of a one-year survey in Kobe, where each plot indicates the NH_3(g) concentration of each biweekly sampling. The NH_3(g) concentration ranged from 0 ppb (N.D.) to around 5 ppb. There were

obvious disparities among the sites in the autumn–spring seasons, especially in the winter; in contrast, the disparities among the sites were relatively small in the summer.

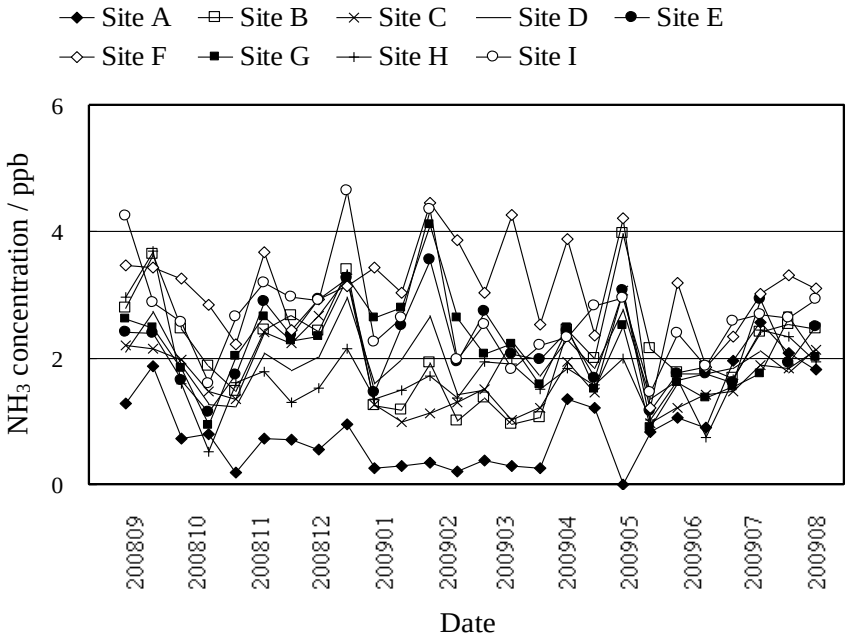

Figure 2.4. Variation of NH_3(g) concentration in one-year sampling period at survey sites in Kobe.

This monthly and seasonal disparity are expected to be partially explained by a vertical mixing (convection) and a horizontal transport (advection) due to meteorological conditions: a smaller seasonal variation in wind speed (Autumn: 3.6 m/s, Winter: 3.6, Spring: 3.5 and Summer: 3.3) and a larger seasonal variation in air temperature (Autumn: 19.6°C, Winter: 8.1, Spring: 15.0 and Summer: 26.0). The smaller seasonal variation in wind speed would create a favorable condition for non-seasonal air advection, and the larger seasonal variation in air temperature would lead to a large seasonal difference in vertical air mixing; that is, more active convection in the summer. Therefore, under high temperature in the summer, the fate of NH_3(g) at the surface was dominated by relatively enhanced convection (vertical mixing) and then NH_3(g) horizontally transported throughout the area homogenously by non-seasonal advection, causing the small disparities among the sites in the summer, which could not be seen in the cool dominated period (autumn-spring).

Figure 2.5 shows the seasonal variation of the NH_3(g) concentration among the sites in Kobe, where the difference in the NH_3(g) concentrations between the seasonal mean and the annual mean, i.e., subtracting the annual mean from the seasonal mean, is plotted in the vertical axis. Based on conventional wisdom in studies about atmospheric ammonia, there is a common confirmation that the NH_3(g) concentration tends to peak during warmer seasons of summer, while dropping to the minimum during colder seasons like winter. This type of warm period dominance has been observed from several studies conducting in various countries (Yamamoto et al., 1995; Lee et al., 1999; Bari et al., 2003; Walker et al., 2004; Day et al., 2012; Hu et al., 2014; Chang et al., 2016; Wu et al., 2018; Wang et al., 2018). However, it was different in this study, i.e., except for Site A, the NH_3(g) concentration in the summer was lower than the annual mean at all sites and lower than those in other seasons at most of the sites.

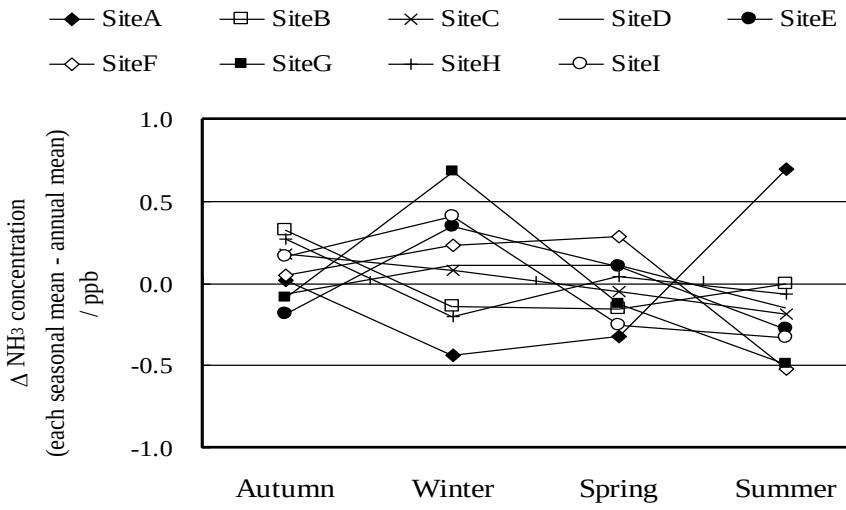

Figure 2.5. Seasonal variation of NH_3(g) concentration among the survey sites in Kobe. Difference of the NH_3(g) concentration between the seasonal mean and the annual mean: the seasonal mean – the annual mean is plotted in the vertical axis.

This correlation of no significance between ambient temperature and the NH_3(g) concentration has hardly ever been found in numerous places; nevertheless, not only this extraordinary finding was observed at Kobe sampling sites, but it was also detected at Kitakyushu survey site. Figure 2.6 illustrates the monthly NH_3(g) concentration along with

ambient temperature at Kitakyushu site, in which, an only minus value detected in March was replaced to zero in the calculation of monthly mean concentration. Based on the Fig. 2.6, in Kitakyushu, the NH_3(g) concentration was getting lower continuously (around 3.5 ppb) in the warm period (more than 20ºC) from August to October, especially in August, when the air temperature reached the peak in summer of almost 30ºC. Aikawa et al. (2005a), and Aikawa and Hiraki (2008) studied the concentrations of NH_3(g) and NH_4^+(p) at Site C by using a detailed 4-stage filter-pack method. In their studies, the total concentration of NH_3(g) and NH_4^+(p) showed a seasonal variation: summer > (autumn, spring) > winter. Despite the higher total concentration in the summer in their studies, the NH_3(g) concentration in our present study was lower in the summer. Aikawa and Hiraki (2008) further studied the acid-base balance of acid-related (HNO_3, NO_3^- and non-sea-salt-(nss-)SO_4^{2-}) and alkali-related (NH_3, NH_4^+ and nss-Ca^{2+}) chemical species at Site C, and they clarified that the acid-related species were comparable to the alkali-related species in the summer, while the alkali-rich distribution was pronounced in the winter. This means that acid-related species would generally be higher in the summer than in other seasons (Aikawa and Hiraki, 2008), which is likely responsible for the lower NH_3(g) concentration in the summer than in other seasons through atmospheric chemical reactions. However, for further scientific discussion and a better understanding of the seasonal variation of NH_3(g) concentration, it is necessary to measure other gases and aerosols at the present/other survey sites, including Site C in the future.

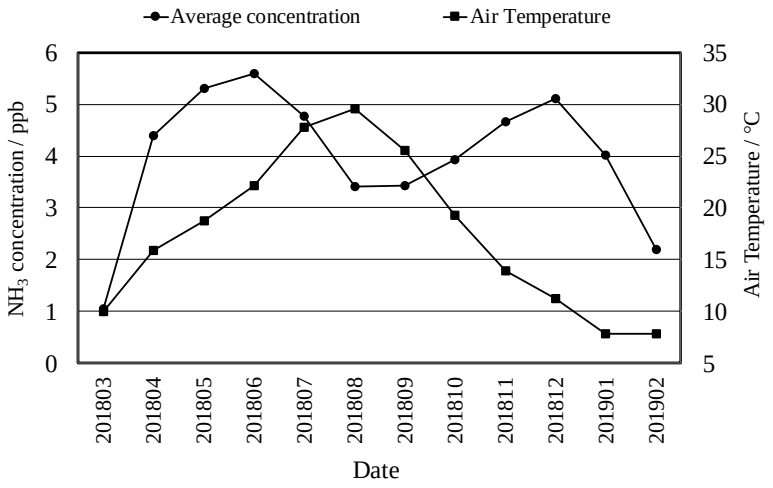

Figure 2.6. Monthly variation of NH_3(g) concentration and ambient temperature at the survey site in Kitakyushu.

Another possible contribution to this seasonal variation, i.e., lower in the summer, is the atmospheric stability. The atmosphere is more unstable in the summer due to the strong solar radiation, which is responsible for the active vertical mixing of the air and triggers the chemical reactions among NH_3(g) and other species in the air. Gong et al. (2011) conducting research about diurnal variation of NH_3(g) also claimed that some sinks related to the intense photochemical processes under the strongest solar radiation in the middle of the day is a likely explanation for the noticeable decrease at mid-day. The stability of the atmosphere well explains the seasonal variation in the current survey; further is consistent with the relatively smaller disparities among the sites in the summer (Fig. 2.4) mentioned and discussed in the first paragraph of this section.

Interestingly, not only undergoing the downtrend in warm period, but the NH_3(g) concentration at Kobe sites also likely experienced the higher level in the colder seasons like winter and autumn at most of the sites except for agriculture-based Site F and D with spring being the highest (detailed discussion in the later part of this section). This phenomenon was also observed at Kitakyushu site, where the concentration remained at a relatively high level of 5 ppb in December (winter) when the temperature was under a low level of around 10°C. In winter, engines more frequently run under high-load conditions in order to reach and maintain

the optimal operating temperature, which potentially induces fuel-rich combustion which favors reducing processes on the catalyst surface. As a result, more NH_3(g) is produced in vehicle exhaust (Heeb et al., 2006; Li et al., 2006), being partially responsible for the higher NH_3(g) concentration in the winter.

Only at Site A, the NH_3(g) concentration in the summer was distinctly higher than those in other seasons. The negligible contribution of vehicular emissions due to the zone restriction of this area being forest in national park might be responsible for non-elevated concentration in the colder seasons. More importantly, a meteorological parameter of wind speed would be presumably attributable to this specific seasonal variation at Site A. The mean wind speeds around Site A were 4.2 m/s (autumn), 5.0 (winter), 4.8 (spring) and 3.8 (summer); this seasonal variation in wind speed was inversely related with the NH_3(g) concentration. A study of Chang et al. (2016) also showed a highly significant relation between wind speed and NH_3(g) concentration, in which the highest average concentrations were measured under the lowest wind speeds and the lowest concentrations were measured at the highest wind speeds. The wind speed was one of the most significant parameters to control the NH_3(g) concentration around Site A because the distinctly high situation (800 meters) of Site A could probably separate this site from other sites in terms of impact factors.

The NH_3(g) concentration at Sites D and F were highest in the spring, while those at many sites were highest in the autumn or the winter. Genfa et al. (1989) and Hu et al. (2014) reported that the concentration of gaseous ammonia was high in the spring due to agricultural activities and fertilizer use. Misselbrook et al. (2000) and Erisman et al. (2008) claimed that agriculture accounted for most of the emission of gaseous ammonia into the atmosphere. The contribution of agriculture to the NH_3 inventory was large at Sites D and F, especially at Site F (discussion in the Section 2.2.4). Therefore, agricultural activities would be associated with the specific seasonal variation at Sites D and F, especially at Site F.

2.3.3. **Spatial distribution**

The annual mean NH_3(g) concentration at each site in Kobe is summarized in Table 2.3. The highest annual mean NH_3(g) concentration was observed at Site F (3.10 ppb), followed by the second position of Site I (2.70 ppb). The group of Site B, C, D, E, G and H illustrated the middle values of annual mean concentration at around 2.00 ppb; and the lowest was at Site A (0.91 ppb).

Table 2.3. Annual mean NH_3(g) concentrations at each site in Kobe. Unit: ppb

Site A	Site B	Site C	Site D	Site E	Site F	Site G	Site H	Site I
0.91	2.12	1.75	1.95	2.22	3.10	2.19	1.76	2.70

The annual mean NH_3(g) concentration at Site A was lower than those at all of other sites, with a statistical significance (p<0.001); that at Site F was higher than those at other sites, with a statistical significance (p<0.001 for sites except for Site I, p<0.05 for Site I). The NH_3(g) concentration at Site F was higher than those at other sites for nearly a year; on the other hand, that at Site A was lowest except for several values in the summer.

Figure 2.7 shows the spatial distribution of the annual mean NH_3(g) concentration in Kobe. The lowest concentration (0.91 ppb) was observed at the site near the summit of Mt. Rokko (Site A), which is in the highest situation of approximately 800 meters a.s.l. and covered mostly by the forest (83 percent). The rougher surface of forest is the reason explaining the dry deposition of ammonia here is higher than on a meadow or other places (Andersen and Hovmand, 1999). The turbulence above a forest is normally higher than that over short vegetation at a certain wind velocity. The deposition velocities are mainly determined by the turbulent transfer; therefore, the deposition rates are larger for the forest than for the short vegetation. In addition, frequent fog events were observed around Site A (Aikawa et al, 2001; 2005b; 2007a; 2007b). Taking that NH_3(g) can easily dissolve into water into account (Asman, 1995), the frequent fog events around Site A is one of the reasons for the lower NH_3(g) concentration around Site A by the scavenging through wet deposition process.

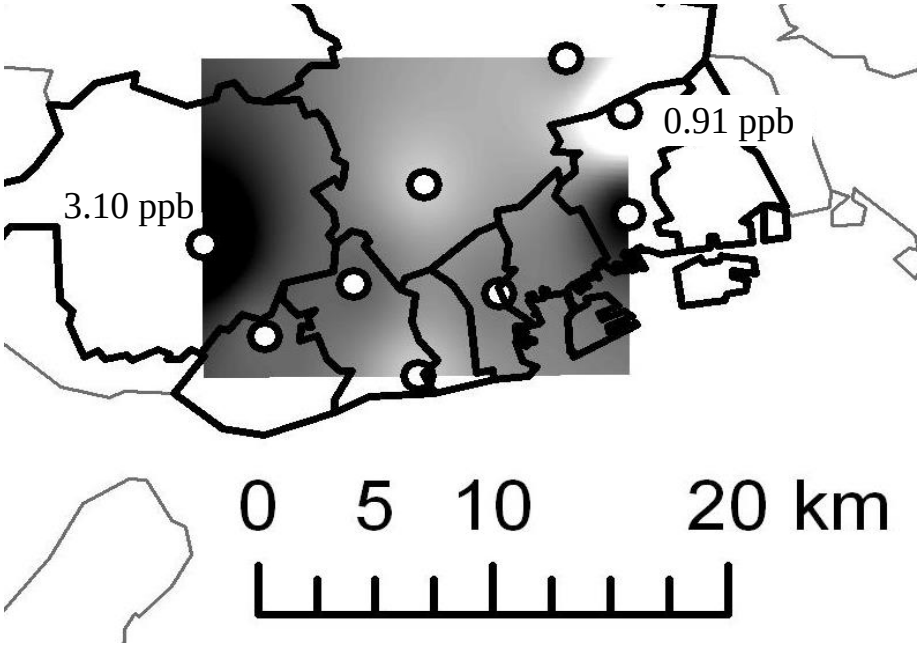

Figure 2.7. Spatial distribution of annual mean NH_3(g) concentration in Kobe.

On the contrary to Site A, the annual mean NH_3(g) concentration at Site F, where the surrounding area is covered with forest (68 percent) in a pretty similar feature to the area around Site A, was the highest (3.10 ppb). The distinguished point is that the second largest proportion of the area around Site F includes enormous emission sources like paddy fields, agriculture, and traffic while Site A is not. Another factor also responsible for the difference between Site A and F is the elevation of setting samplers which are 800 and 85 meters, respectively. The characteristic of the high elevation directly relates to a more active turbulent diffusion due to a larger wind speed. The annual mean wind speed around A during this survey (4.5 m/s) was actually 2.5 times as large as that around C (2.0 m/s) at the elevation of 5 meters, which can be representative of Site F because of the negligible disparity of their sampling elevation. Furthermore, with a view to getting overall insight into the significance of elevation as a controlling factor around the sampling area, the relationship of the annual mean NH_3(g) concentration with the elevation of the sites in Kobe was evaluated and showed in Figure 2.8. A statistically significant correlation ($r=-0.74$, $p<0.05$) was observed. However, if Site A is excluded, the correlation coefficient would become low ($r=-0.37$) and not statistically

significant (p>0.05). Thus, the elevation itself of the site would not be a definite parameter for controlling the concentration of NH_3(g) around this survey area in Kobe except for Site A.

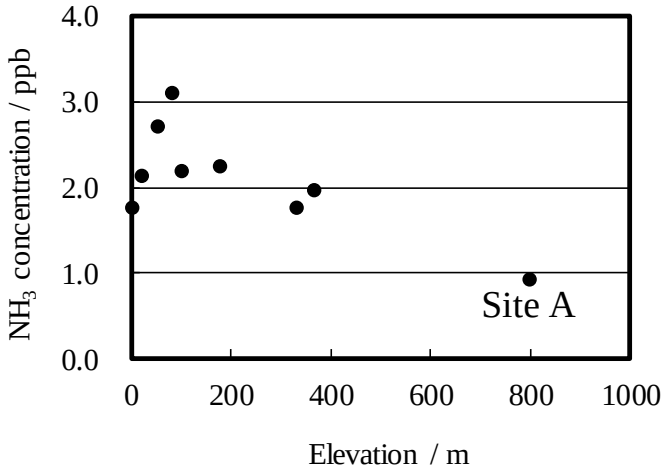

Figure 2.8. Relationship of annual mean NH_3(g) concentration with elevation of each survey site in Kobe.

The highest concentration of NH_3(g) in Site F might be responsible for the relatively high NH_3(g) concentration in Site E (2.22 ppb) and Site G (2.19 ppb) because the magnitude of the horizontal transport, indicating that areas with high emissions can influence the magnitude of the concentration of adjacent or neighboring regions (Dennis et al., 2010).

On the other hand, in areas other than those around Sites A and F, the largest proportion is occupied by the building, although the proportion largely varies from 44 percent (Site D) to 86 percent (Site I). In the eastern region, the NH_3(g) concentration was the second highest (2.70 ppb) in the highly urbanized site (Site I) with a highly concentrated density of residential areas and traffic system, i.e., building and traffic account for 99 percent of the coverage land use, which have been recently estimated as minor sources of ammonia emissions in general but considerable factors in urban atmospheric evaluation. This might also partly explain why the NH_3(g) concentration at Site B, owning the similar features of highly urbanized area to Site I, was 2.12 ppb. Equally important, Site C is also determined as a light-industrial and residential area; putting Site C in a comparison with Site B and I just mentioned above, it is obvious to

see a little lower proportion of land use in terms of building while the proportion of traffic is higher. However, the NH_3(g) concentration at this site was the second lowest (1.75 ppb). The suspected controlling factor at Site C is suggested to be vicinity right next to the open coast. The land/sea breeze circulation generated by a large thermal contrast between the ocean and the land in day time and night time would be associated with many processes that contribute to the trapping and/or dilution of pollution (Bachvarova et al., 2018; Wu et al., 2018), which can also create a favorable condition for the dry deposition of NH_3(g) being highly soluble gas to the seawater surface (Asman and Berkowicz, 1994), which could reduce the NH_3(g) concentration here. Thus, the land use is crucial and could be a likely parameter, accounting for the NH_3(g) concentration considerably well; however, land use cannot absolutely account for the NH_3(g) concentration only by itself.

2.3.4. **Relationship with NH_3 inventory**

The emission inventory of NH_3 based on 1 km x 1 km resolution hourly basis for Japan was developed by Kannari et al. (2007), namely EAGrid2000-japan, was used to analyze the correlation between the measured NH_3(g) concentration and NH_3 inventory. Figure 2.9 shows the relationship of the annual mean NH_3(g) concentration with the total NH_3 emission in Kobe.

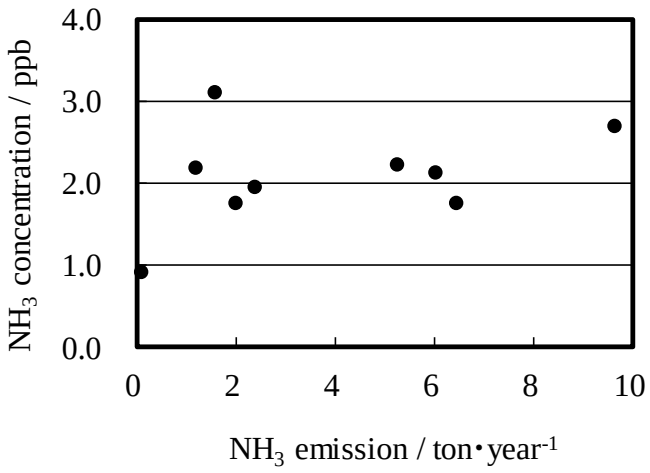

Figure 2.9. Relationship of annual mean NH_3(g) concentration with total NH_3 emission in Kobe.

The correlation between the measured NH_3(g) concentration and the total NH_3 emission was not statistically significant ($r=0.36$, $p>0.05$). So, it seems likely that the total NH_3 emission does not appropriately account for the NH_3(g) concentration.

Our present study was carried out in highly urbanized areas, in which quantifying the magnitude of NH_3 emissions is more uncertain than for agricultural sources (Murano et al., 1995; Sutton et al., 2000). Yokoyama et al. (2002) reported that the emission strength of gaseous ammonia in urban areas corresponded to that from livestock. The NH_3 emission from each emission source in Kobe is categorized in Figure 2.10.

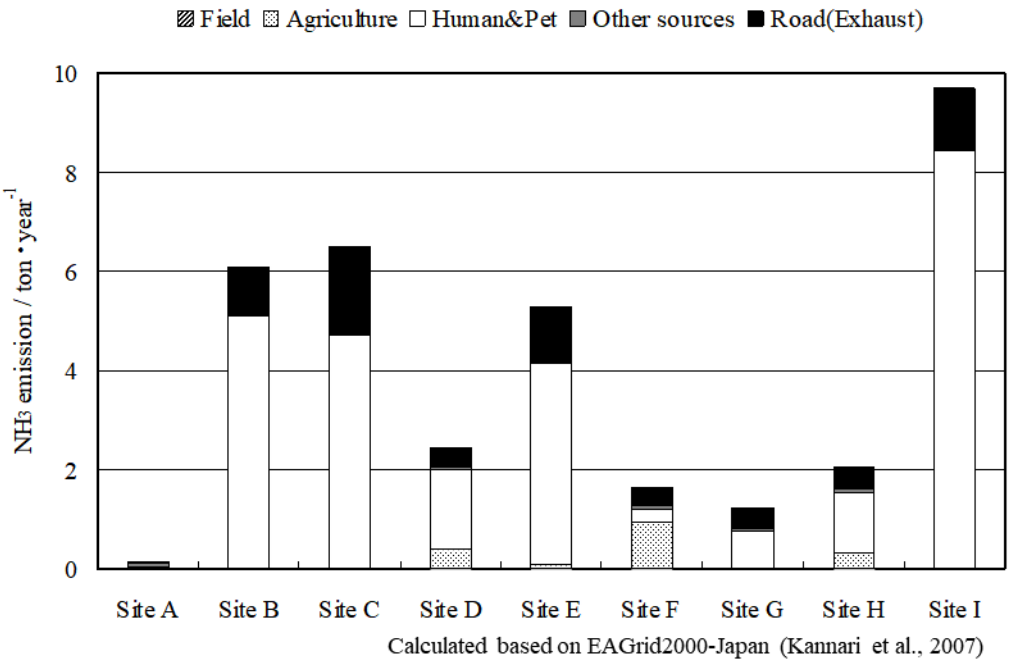

Figure 2.10. NH_3 emission from each emission source in NH_3 inventory in Kobe.

The source of Human&Pet accounts for the largest proportion in NH_3 inventory, followed by Road (Exhaust) in most of the areas, with the exception of Sites A and F because Other sources and Agriculture take up the largest proportion of NH_3 emission in the area around Site A and F, respectively. Here, the emission from Human&Pet was based on the statistical activity data of the population and the registered number of dogs (Kannari et al., 2007). Figure 2.11(a) shows the relationship of the annual mean NH_3(g) concentration with the proportion of

Human&Pet to the total NH_3 emission in the NH_3 inventory. The correlation was not statistically significant (r=0.20, p>0.05). Figure 2.11(a) shows that Site F was anomalously plotted. If Site F is supposedly excluded from Fig. 2.11(a), the correlation would become statistically significant (r=0.90, p<0.01). As described above, the contribution of Agriculture in the area around Site F is larger than those at other sites, so the exclusion of Site F in Fig. 2.11(a) provides a statistically significant (r=0.90, p<0.01) correlation. On the other hand, in discussing the relationship between the annual mean NH_3(g) concentration and the elevation of the survey site (Section 3.2.2), the existence of Site A resulted in a statistically significant correlation; therefore, the existence of Site A should be evaluated in Fig. 2.11(a). The correlation coefficient was large (r=0.67), although it was not statistically significant (p>0.05). However, the linear approximation equations were as follows:

(NH_3(g) concentration) = 2.07 x (Proportion of Human&Pet) + 0.60: with the exception of Site F.

(NH_3(g) concentration) = 2.09 x (Proportion of Human&Pet) + 0.58: with the exceptions of Site A and F.

Both the slope and the intercept in the approximation equations were quite similar; therefore, the application of the proportion of Human&Pet to the total NH_3 emission would be an effective parameter for potentially accounting for the NH_3(g) concentration.

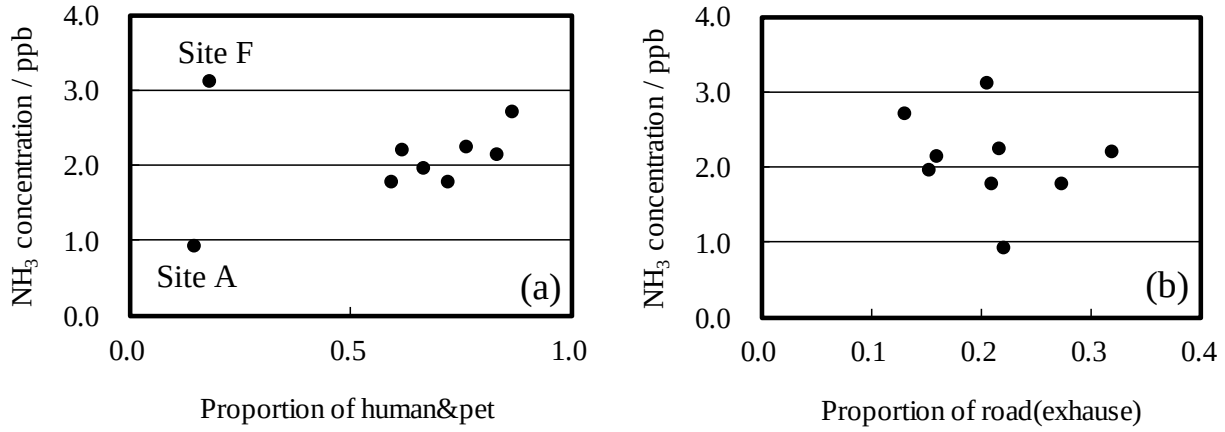

Figure 2.11. Relationships of annual mean NH_3(g) concentration with the proportion of Human&Pet (a) and Road (Exhaust) (b) to the total NH_3 emission in NH_3 inventory in Kobe.

In the case of the Road (Exhaust), which showed the second largest contribution in the NH_3 inventory, there was no statistically significant correlation being observed; moreover, there was no anomalous plot (Figure 2.11(b)) as there was for Human&Pet (Fig. 2.11(a)). Thus, when discussing the NH_3(g) concentration in an urbanized area, as in our present study area, the proportion of Human&Pet to the total could provide a good correlation with the NH_3(g) concentration if the contribution of Agriculture is sufficiently taken into account.

2.4.**Conclusions**

The NH_3(g) concentrations were measured using the passive sampling method in two regions of Japan, which are Kobe, where urbanized and agricultural areas are located along with a mountainous area within a 20-km x 20-km range; and typical urbanized and industrialized area in Kitakyushu. The annual mean NH_3(g) concentration was 2.08±0.9 ppb (range from 0 ppb to around 5 ppb) in Kobe, and 4.28±1.7 ppb in Kitakyushu (range from 0 to 8.94 ppb). The NH_3(g) concentrations were discussed from the viewpoint of temporal variations (monthly and seasonal basis). The summer had the lower concentration than other seasons at most of the sites while higher concentration was seen in the colder period, also the lower level of atmospheric stability in summertime was a contributor to the homogeneity of

the NH_3(g) concentration in entire sampling region of Kobe. In terms of spatial distribution, the agricultural area indicated the highest concentration regardless of any other controlling factors, followed by highly commercial and residential areas; whereas the mountainous area witnessed the lowest. Furthermore, effective parameters accounting for the NH_3(g) concentration were studied from the viewpoint of site location (the elevation of the sites), land use around the sites, meteorological condition and the NH_3 inventory. As a result, wind speed was one of the most significant parameters to account for the specific seasonal variation observed at high-elevation site, and multiple controlling factors were mutually related and contributed to the seasonal variation at the sites located in the urbanized areas. In addition, the contribution of Human&Pet in the NH_3 inventory could most effectively account for the NH_3(g) concentration if the contribution of agriculture and the meteorological situation are sufficiently considered.

References

Aikawa, M. and Hiraki, T. (2008). Methodology of analysis associating survey results by the filter-pack method with those of precipitation - Acid-base balance on acid-related and alkali-related chemical species in urban ambient air and its influence on the acidification of precipitation. *Journal of Atmospheric Chemistry* **61**: 21-29. https://doi.org/10.1007/s10874-009-9122-9.

Aikawa, M., Hiraki, T. and Tamaki, M. (2005a). Characteristics in concentration of chemical species in ambient air based on three-year monitoring by filter pack method. *Water, Air and Soil Pollution* **161**: 335 – 352. https://doi.org/10.1007/s11270-005-4774-9.

Aikawa, M., Hiraki, T., Mukai, H. and Murano, K. (2008). Characteristic variation of concentration and chemical form in sulfur, nitrate, ammonium, and chloride species observed at urban and rural sites of Japan. *Water, Air and Soil Pollution* **190**: 287-297. https://doi.org/10.1007/s11270-007-9600-0.

Aikawa, M., Hiraki, T., Shoga, M. and Tamaki, M. (2001). Fog and precipitation chemistry at Mt. Rokko in Kobe, April 1997-March 1998. *Water, Air and Soil Pollution* **130**: 1517-1522. https://doi.org/10.1023/A:1013945905410.

Aikawa, M., Hiraki, T., Shoga, M. and Tamaki, M. (2005b). Chemistry of fog water collected in the Mt. Rokko area (Kobe City, Japan) between April 1997 and March 2001. *Water, Air and Soil Pollution* **160**: 373-393. https://doi.org/10.1007/s11270-005-3117-1.

Aikawa, M., Hiraki, T., Shoga, M., Tamaki, M. and Sumitomo, S. (2007a). Seven-year trend of the time and seasonal dependence of fog water collected near an industrialized are in Japan. *Atmospheric Research* **83**: 1-9. https://doi.org/10.1016/j.atmosres.2006.01.011.

Aikawa, M., Hiraki, T., Suzuki, M., Tamaki, M. and Kasahara, M. (2007b). Separate chemical characterizations of fog water, aerosol, and gas before, during, and after fog events near

an industrialized area in Japan. *Atmospheric Environment* **41**: 1950-1959. https://doi.org/10.1016/j.atmosenv.2006.10.049.

Andersen, H. V. and Hovmand, M. F. (1999). Review of dry deposition measurements of ammonia and nitric acid to forest. *Forest Ecology and Management* **114(1)**: 5–18. https://doi.org/10.1016/S0378-1127(98)00378-8.

Asman, W. A. H. (1995). Parameterization of below-cloud scavenging of highly soluble gases under convective conditions. *Atmospheric Environment* **29(12)**: 1359–1368. https://doi.org/10.1016/1352-2310(95)00065-7.

Asman, W. A. H. and Berkowicz, R. (1994). Atmospheric nitrogen deposition to the North Sea. *Marine Pollution Bulletin*, **29(6–12)**: 426–434. https://doi.org/10.1016/0025-326X(94)90666-1.

Bachvarova, E., Spasova, T. and Marinski, J. (2018). Air Pollution and Specific Meteorological Conditions at the Adjacent Areas of Sea Ports. *IFAC-PapersOnLine,* **51(30)**: 378–383. https://doi.org/10.1016/j.ifacol.2018.11.336.

Bari, A., Ferraro, V., Wilson, L. R., Luttinger, D. and Husain, L. (2003). Measurements of gaseous HONO, HNO_3, SO_2, HCl, NH_3, particulate sulfate and PM2.5 in New York, NY. *Atmospheric Environment* **37(20)**: 2825–2835. https://doi.org/10.1016/S1352-2310(03)00199-7.

Chang, Y., Zou, Z., Deng, C., Huang, K., Collett, J. L., Lin, J., Zhuang, G. (2016). The importance of vehicle emissions as a source of atmospheric ammonia in the megacity of Shanghai. *Atmospheric Chemistry and Physics* **16(5)**: 3577–3594. https://doi.org/10.5194/acp-16-3577-2016.

Day, D. E., Chen, X., Gebhart, K. A., Carrico, C. M., Schwandner, F. M., Benedict, K. B., Schichtel, B. A. and Collett, J. L. (2012). Spatial and temporal variability of ammonia and

other inorganic aerosol species. *Atmospheric Environment* **61**: 490–498. https://doi.org/10.1016/j.atmosenv.2012.06.045.

Dennis, R. L., Mathur, R., Pleim, J. E. and Walker, J. T. (2010). Fate of ammonia emissions at the local to regional scale as simulated by the Community Multiscale Air Quality model. *Atmospheric Pollution Research* **1(4)**: 207–214. https://doi.org/10.5094/APR.2010.027.

Erisman, J. W., Bleeker, A., Hensen, A. and Vermeulen, A. (2008). Agricultural air quality in Europe and the future perspectives. *Atmospheric Environment* **42(14)**: 3209–3217. https://doi.org/10.1016/j.atmosenv.2007.04.004.

Genfa, Z., Dasgupta, P.K. and Dong, S. (1989). Measurement of atmospheric ammonia. *Environmental Science and Technology* **23**: 1467-1474. https://doi.org/10.1021/es00070a003.

Heeb, N. V., Forss, A.-M., Brühlmann, S., Lüscher, R., Saxer, C. J. and Hug, P. (2006). Three-way catalyst-induced formation of ammonia- velocity- and acceleration-dependent emission factors. *Atmospheric Environment* **40(31)**: 5986–5997. https://doi.org/10.1016/j.atmosenv.2005.12.035.

Hu, Q., Zhang, L., Evans, G. J., Yao, X. (2014). Variability of atmospheric ammonia related to potential emission sources in downtown Toronto, Canada. *Atmospheric Environment* **99**: 365-373. https://doi.org/10.1016/j.atmosenv.2014.10.006.

Japan Environmental Laboratories Association (2017). Acid deposition survey in Japan, Phase 5 (Fiscal Year 2015). *Journal of Environmental Laboratories Association* **42(3)**: 83-126. (in Japanese).

Kannari, A., Tonooka, Y., Baba, T. and Murano, K. (2007). Development of multiple-species 1 km x 1 km resolution hourly basis emissions inventory for Japan. *Atmospheric Environment* **41**: 3428-3439. https://doi.org/10.1016/j.atmosenv.2006.12.015.

Kobe City (2008). http://kobe-taikikanshi.jp/kankyo/download/month/Downloadmonth_2008.html (last access 2018.10.14.).

Kobe City (2009). http://kobe-taikikanshi.jp/kankyo/download/month/Downloadmonth_2009.html (last access 2018.10.14.).

Lee, H. S., Kang, C.-M., Kang, B.-W. and Kim, H.-K. (1999). Seasonal variations of acidic air pollutants in Seoul, South Korea. *Atmospheric Environment* **33(19)**: 3143–3152. https://doi.org/10.1016/S1352-2310(98)00382-3.

Li, Y., Schwab, J. J. and Demerjian, K. L. (2006). Measurements of ambient ammonia using a tunable diode laser absorption spectrometer: Characteristics of ambient ammonia emissions in an urban area of New York City. *Journal of Geophysical Research: Atmospheres* **111(D10)**: n/a-n/a. https://doi.org/10.1029/2005JD006275.

Misselbrook, T. H., Van Der Weerden, T. J., Pain, B. F., Jarvis, S. C., Chambers, B. J., Smith, K. A., Phillips, V. R. and Demmers, T. G. M. (2000). Ammonia emission factors for UK agriculture. *Atmospheric Environment* **34**: 871-880. https://doi.org/10.1016/S1352-2310(99)00350-7.

Murano, K., Hatakeyama, S., Mizoguchi, T. and Kuba, N. (1995). Gridded ammonia emission fluxes in Japan. *Water, Air, and Soil Pollution* **85**: 1915-1920. https://doi.org/10.1007/BF01186114.

Sutton, M. A., Dragosits, U., Tang, Y. S. and Fowler, D. (2000). Ammonia emissions from non-agricultural sources in the UK. *Atmospheric Environment* **34**: 855-869. https://doi.org/10.1016/S1352-2310(99)00362-3.

Walker, J. T., Whitall, D. R., Robarge, W. and Paerl, H. W. (2004). Ambient ammonia and ammonium aerosol across a region of variable ammonia emission density. *Atmospheric Environment* **38(9)**: 1235–1246. https://doi.org/10.1016/j.atmosenv.2003.11.027.

Wang, C., Yin, S., Bai, L., Zhang, X., Gu, X., Zhang, H., Lu, Q and Zhang, R. (2018). High-resolution ammonia emission inventories with comprehensive analysis and evaluation in Henan, China, 2006–2016. *Atmospheric Environment* **193**: 11–23. https://doi.org/10.1016/j.atmosenv.2018.08.063.

Wu, S.-P., Dai, L.-H., Wei, Y., Zhu, H., Zhang, Y.-J., Schwab, J. J., Yuan, C.-S. (2018). Atmospheric ammonia measurements along the coastal lines of Southeastern China: Implications for inorganic nitrogen deposition to coastal waters. *Atmospheric Environment* **177**: 1-11. https://doi.org/10.1016/j.atmosenv.2017.12.040.

Yamamoto, N., Nishiura, H., Honjo, T., Ishikawa, Y. and Suzuki, K. (1995). A long-term study of atmospheric ammonia and particulate ammonium concentrations in Yokohama, Japan. *Atmospheric Environment* **29(1)**: 97–103. https://doi.org/10.1016/1352-2310(94)00226-B.

Yokoyama, S., Oshio, T. and Hara, H. (2002). Emission of acidification chemical species in Chiba Prefecture (5) – Comparison of emission sources in urban area and rural area-. *Proceedings of the 43rd Annual Meeting of the Japan Society for Atmospheric Environment*: 398. (In Japanese).

Chapter 3. Characteristics of ambient NH_3(g) concentration in downtown in Hanoi and its suburbs in Vietnam

3.1. Introduction

Vietnam has been experiencing rapid economic development (Hien et al., 2020). Based on the Environmental Performance Index (2012) released at the World Economic Forum in Davos, Vietnam is one of the top ten countries that suffer from the worst air pollution in the world (Hien et al., 2014). Hanoi, the capital city, is the most polluted urban area in the country because the uncontrolled growth of construction works, high-density traffic, and small manufacturing activities has resulted in an increasing number of air pollution sources (Cohen et al., 2010). Most prior studies on air pollution in Hanoi focused on particulate matters (Hien et al., 2002; Kim Oanh., 2006; Hopke et al., 2008; Cohen et al., 2010) rather than exploring gaseous pollutants (Hien et al., 2014; Sakamoto et al., 2018). Although it is common to find data on regulated air pollutants (e.g., $PM_{2.5}$, PM_{10}, SO_2, NO_2, and CO) over the years from the governmental institutions' reports (Ministry of Natural Resources and Environment, 2014; 2016; 2017), the data on NH_3(g) in Hanoi, as its measurement is not mandatory in the regulatory framework, is unprecedented.

This research was designed to address the shortage of NH_3(g) data in Vietnam in general and Hanoi in particular. This is the first comprehensive and temporally continuous NH_3(g) measurement at multiple sites in Hanoi, Vietnam, during one-year period of four seasons. In addition to spatial distribution, the seasonal variation of NH_3(g) concentrations was thoroughly discussed, together with meteorological parameters. We attempted to further identify the major sources and controlling factors responsible for the higher concentrations registered in certain areas of the city. Furthermore, this research will pave the way for further studies relative to atmospheric environmental pollution in Vietnam thanks to the experience in conducting experiments with long-range delivery.

3.2. Experimental

3.2.1. Survey site

There are two key target areas, urban and suburban area in Hanoi, Vietnam. Hanoi is the second largest urban agglomeration in Vietnam. The area of Hanoi is around 3,359 square kilometers, with a total population of nearly 7.3 million people, i.e., the population density is approximately 2,182 people per square kilometer (General Statistics Office, 2016). To determine the spatial distribution of NH_3(g) concentrations, source-specific monitoring campaigns were designed focusing on the impact of traffic, a polluted river, a downtown area, and a rural site on NH_3(g) concentration. There were four sampling sites, including three in an urbanized area, namely Thanh Xuan district, and one in a suburban area (Fig. 3.1):

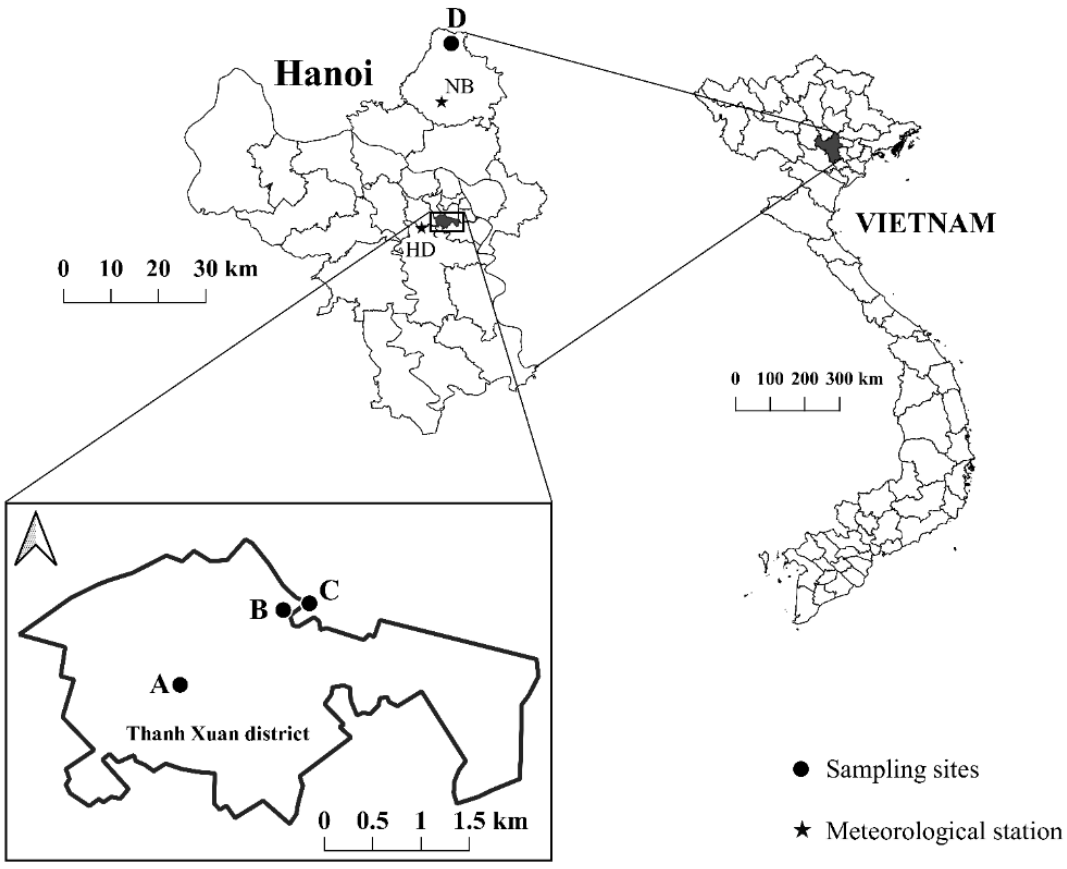

Figure 3.1. Location map of sampling sites and meteorological stations in Hanoi.

Site A: Site A was established at Hanoi University of Science (HUS), which is representative of a typical outdoor environment in the urbanized area of Hanoi. This site is assumed to be under the total influence of numerous emission sources instead of a particular impact from a specific one.

Site B: Site B was established at the bank of the To Lich River, which is the most polluted river in the urban area, having a function of an open drainage.

Site C: Site C was established at an intersection with a high-density traffic load.

Site D: Site D was established in an atmosphere typical of a suburban area in the Soc Son district, with agricultural fields nearby.

The characteristics of each site are summarized in Table 3.1. The sampler was installed at a height of ca. 1.5 meters above the ground.

Table 3.1. Survey sites in Hanoi.

Sites	Latitude	Longitude	Zone restrictions
Site A	20°59'43.0"N	105°48'29.3"E	Representative urban area
Site B	21°00'10.2"N	105°49'12.8"E	Open wastewater body
Site C	21°00'07.4"N	105°49'03.4"E	High traffic density
Site D	21°21'13.8"N	105°49'36.9"E	Representative suburban area

3.2.2. Sampling period and seasonal classification

The sampling period was one year, from March 2018 to February 2019, on a weekly basis at Site A (hereafter referred to as weekly samples). Intensive sampling was also conducted on a daily basis within one week with exemplary meteorological characteristics of a season at all survey sites (hereafter referred to as daily samples). There are four seasons in Hanoi: spring (March, April, and May), summer (June, July, and August), autumn (September, October, and November), and winter (December, January, and February). However, because the change in meteorological characteristics is not clear enough to determine a week symbolic of autumn, the

sampling time during the transitional period in October was necessarily additional. Thus, there is a total of six daily-basis sampling periods:

Spring: March 5 to March 11, 2018, at all sites;

Summer: July 2 to July 8, 2018, at all sites;

Transition 1: October 2 to October 8, 2018, at sites A, B, and C;

Transition 2: October 15 to October 21, 2018, at Site D;

Autumn: November 13 to November 19, 2018, at all sites; and

Winter: January 14 to January 20, 2019, at all sites.

3.2.3. IC Chemical analysis

Deionized water (10 ml) was used in the extraction of the filter paper. The extracts were measured with an ion chromatography system, the Thermo Scientific™ Dionex™ Integrion (Thermo Fisher Scientific, Inc., Massachusetts, USA), for NH_4^+ analysis.

3.2.4. Transportation of device

For the sampling in Hanoi, the transport back and forth of the samplers between Japan and Vietnam was unavoidable. Each sampling device was sealed in a resealable aluminum pouch (RAP), and then all of them were put into a bigger one, which is classified based on each sampling site. Those pouches of samplers were delivered to a coordinated laboratory in Hanoi, where the samplers used for the urban areas (sites A, B, and C) and the suburban area (Site D) were stored at HUS and Soc Son, respectively. All of them were stored in a desiccator before exposure to the environment. The samples were then delivered back to an analytical laboratory in Japan for chemical analysis.

3.2.5. Meteorological parameters

The meteorological data for four parameters, temperature, relative humidity, wind speed, and wind direction during the sampling period, were obtained from the Integrated Surface Database (ISD) of the National Centers for Environmental Information, US National Oceanic and Atmospheric Administration (NOAA), at nearby meteorological stations. The meteorological data used for analysis at sites A, B, and C were obtained from the Ha Dong station (station ID: 488250-99999), and meteorological data from Noi Bai International Airport (station ID: 488200-99999) was used for Site D (Fig. 3.1).

3.3. Results and discussion

3.3.1. Data management for blanks

The blank concentration was subtracted from the concentration of corresponding exposed samples; thus, the blanks are crucial to determining the actual concentration of $NH_3(g)$ at the survey sites and directly affect the accuracy of the results. In this study, the travel blank Type 1 (Table 3.2) was established along with daily and weekly samples for the entire sampling period.

In detail, the blank values of daily samples and weekly samples are shown in Tables 3.3 and 3.4 respectively. There are two blank values higher than the exposed sample concentrations, in which the blank of daily summer at Site D (0.18 mg L^{-1}) was 1.1 times higher than four corresponding samples with a mean of around 0.16 mg L^{-1}, and the blank of weekly sampling in June 2018 (1.39 mg L^{-1}) was 2.9 times higher than all corresponding samples with a mean of ca. 0.48 mg L^{-1}.

Table 3.2. Types of blank.

Types of blank	Container	Characteristics
Type 1	One RAP[a]	One PSD[b] was placed into one RAP and seal closely.
Type 2	Air-tight brown vial	One PSD was placed into an air-tight brown vial and close securely.
Type 3	Three RAPs	One PSD was placed into a small RAP (Type 1), and then was placed into two more layers of bigger RAPs.

[a] RAP: Resealable Aluminum Pouch.

[b] PSD: Passive Sampling Device.

Table 3.3. Blank values of daily samples. Unit: mg L^{-1}

	Spring	Summer	Transition	Autumn			Winter	
Blank types	Type 1	Type 1	Type 1	Type 1	Type 2	Type 3	Type 1	Type 3
Site A	0.0279	0.0500	0.0023	0.0004	**0.0931**	N.D.	0.0124	0.0151
Site B	0.0431	0.0447	0.0029	N.D.	0.0002	N.D.	0.0126	0.0060
Site C	0.0363	0.1135	0.0034	N.D.	**0.0885**	_	0.0045	0.0044
Site D	0.0387	**0.1828**	0.0063	N.D.	0.0002	0.0017	0.0093	0.0062

Note: Bold figures show the higher values than exposed samples.

N.D. shows not detected values by Ion Chromatography analysis.

"_" shows not conducted sample.

For those abovementioned cases, quality assurance and quality control (QA/QC) procedures were conducted as follows: the blank of daily summer at Site D was replaced by the median 0.08 mg L^{-1} of blank values in the summer sampling period, and the blank of weekly sampling in June 2018 was replaced by the median 0.20 mg L^{-1} of blank values in the entire weekly sampling period.

It is obvious that the blank values, even though the samples were kept in the same storage environment, had a high degree of variability, suggesting that stricter QA/QC should be required for precise determination of the NH_3(g) concentration. Therefore, a different set of three kinds of blanks (Table 3.2) in terms of airtightness was applied to the daily sampling of autumn and winter and the weekly sampling of November and December 2018. For such modification, Type 1 predictably showed higher values, especially in the weekly samples. However, Type 2 showed two unusually high values compared with other blank values at that time. This might be due to human-induced errors during the delivery time. With the large size of the brown vial, Type 2 is bulky and may not be recommended for the kind of study requiring long-range delivery. Instead of Type 2, the blank values and variability of Type 3 were lowered significantly in both daily and weekly sampling periods. This approach should help to reduce travel-induced contamination of the samplers and produce more precise data.

Table 3.4. Blank values of weekly samples. Unit: mg L^{-1}

2018												2019				
Mar	Apr	May	Jun	Jul	Aug	Sep	Oct	Nov	Dec			Jan			Feb	
Type 1	Type 1	Type 1	Type 1	Type 1	Type 1	Type 1	Type 1	Type 1	Type 1	Type 2	Type 3	Type 1	Type 2	Type 3	Type 1	Type 3
0.1704	0.2876	0.1662	**1.3949**	0.1013	0.0816	0.2396	0.0515	0.0594	0.2882	0.0246	0.0078	0.2831	0.1067	0.0401	0.4084	0.1249

Note: Bold figures show the higher values than exposed samples.

3.3.2. Spatial variation of concentration

Fig. 3.2(a) and (b) show the daily variation and distribution of NH_3(g) concentration at four sites, respectively. During the sampling periods, Site B almost always had the highest values, with an annual average of ca. 79.8±61.2 ppb, which is nearly two times higher than other sites' concentration. Among the other three sites, in urban area, Site C and Site A has annual mean concentrations of 38.6±18.8 and 36.5±20.0 ppb, respectively. The lowest annual average of 35.6±36.0 ppb was observed at Site D in suburban area.

The highest NH_3(g) concentration (79.8±61.2 ppb) at Site B most likely indicates a huge emission from the polluted river as an important source unheard of in the urban area of Hanoi. The To Lich River is the main open drainage in Hanoi. The main direct discharge to the river is the sewage system on both sides of the river, including mostly domestic wastewater treated by septic tanks and untreated industrial wastewater (Dinh Dap, 2019; Ha et al., 2020). Because the major pollutants were derived from households, nitrogen-rich waste such as organic substances were at a high level, at which the biological oxygen demand (BOD_5) and ammonium nitrogen (NH_4-N) were reported to be 90–110 mg L^{-1} and 40–50 mg L^{-1}, respectively. The release of NH_3(g) from the liquid phase is considered to be a process of convective mass transfer across an aqueous–gaseous interface into a free airstream. Gas is produced in organic wastewater under biological decomposition (i.e., microbial and enzymatic activities), which can convert organic matter into ionized substances (i.e., NH_4^+) and/or free gas (i.e., NH_3) that volatilizes into the atmosphere (Ni et al., 2009).

Internationally, data on NH_3(g) emissions from polluted rivers in urban areas have been scarcely reported and poorly understood; instead, most of the research is on NH_3(g) emission from liquid waste from agricultural sources (i.e., swine lagoon (Aneja et al., 2001; Bajwa et al., 2006) and manure (Dai et al., 2015; Mohammed-Nour et al., 2019).

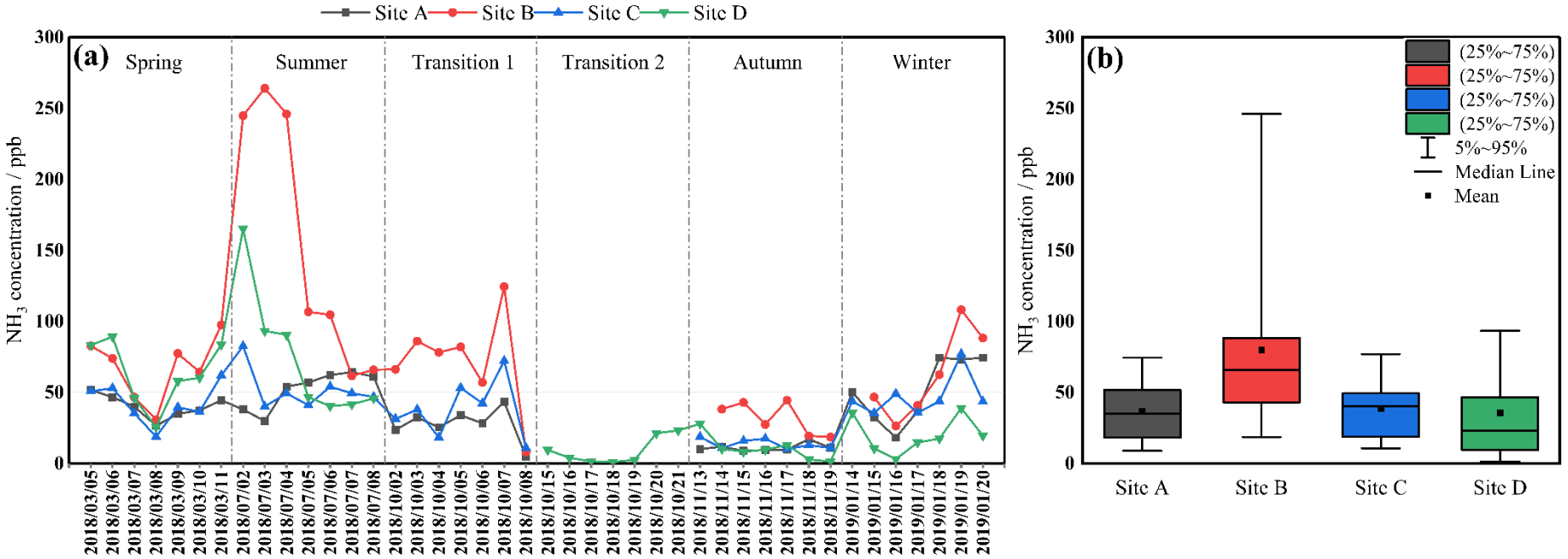

Figure 3.2. Daily variation (a) and distribution (b) of NH_3(g) concentration at four sampling sites based on daily sampling basis in Hanoi.

Several studies of air pollutant emissions from wastewater treatment plants (WWTPs) showed that the emission of ammonia from wastewater is a major source of pollution in urban regions (e.g., Bouwman et al., 1997; Zheng et al., 2012). Thus, the ammonia released from polluted rivers in urban areas needs to be thoroughly investigated in further studies.

Except for Site B, sites A, C, and D experienced a quite similar concentration level (Fig. 3.2(b)). In terms of Site D (35.6±36.0 ppb), the main suspected factor at this site is the agricultural activities nearby. In the Soc Son district, one of the main economy sectors is agricultural production to support the high demand for rice and vegetables in Hanoi. The proportion of agricultural land in Soc Son is about 58.7 percent, and 59.4 percent of the population works in agriculture (Thom, 2013). The impact from agricultural activities and fertilizer use is presumably the reason for the higher concentration in spring and summer than other seasons (see detailed discussion in Section 3.3.3).

In urban area, Site C and Site A has concentrations of 38.6±18.8 and 36.5±20.0 ppb, respectively. The effect of vehicle emission likely explains the concentrations at these two sites. The introduction of three-way catalytic converters is commonly believed to be the cause of NH_3(g) emissions as a byproduct (Livingston et al., 2009; Yao et al., 2013). Therefore, the huge number of personal vehicles - in 2016, there were around 5 million motorbikes (an increase of 6.7% per year from 2011) and 550 thousand cars (an increase rate of 10.2% per year from 2011) (Department of Transport, 2017) - would be mainly responsible for the concentration at these sites. However, the fact that the concentration at Site C was slightly higher than that at Site A could result from different traffic density between an intersection of Site C and typical urbanized area of Site A. The highest NH_3(g) concentration was observed in slow urban traffic (below 20 km h^{-1}) (Heeb et al., 2006), which is a typical characteristic of traffic conditions around the intersection of Site C. In addition, the regular acceleration condition due to the delayed traffic condition at the signalized intersection is conducive to a higher NH_3(g) emission

level than other steady-state conditions (i.e., smooth traffic) because fuel-rich combustion ($\lambda<1$), which prevails when accelerating the vehicle, is attributed to the formation of NH_3 in the catalyst (Huai et al., 2003; Livingston et al., 2009).

3.3.3. Temporal variation and relationship with meteorological parameters

Seasonal variation based on daily sampling at sites A, B, C, and D

In this part, the NH_3(g) concentration in autumn is adapted by the mean value of concentrations in the transition and autumn sampling periods described in Section 3.2.2. The seasonal variations in concentration at the four sites based on daily sampling is shown in Figure 3.3. At sites B and D, the highest concentration was observed in summer, followed by spring, and winter and autumn had similarly low concentrations.

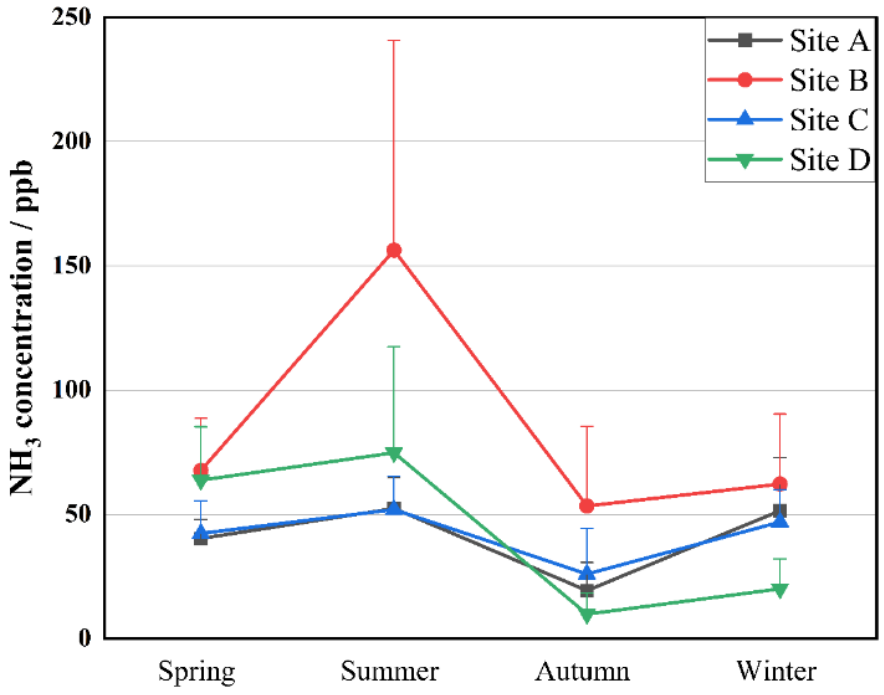

Figure 3.3. Seasonal variation in NH_3(g) concentration of daily sampling basis in Hanoi. Dot represents the mean concentration. Whisker shows the standard deviation. Note: to avoid difficulty to see by overlapping, whiskers are drawn only at the upper side of the dots.

Positive correlations of NH_3(g) concentration with temperature were found to be statistically significant at these two sites, with $p < 0.001$ at Site B and $p < 0.01$ at Site D (Table 3.5), which strongly indicates the significant effect of ambient temperature on the change in NH_3(g) concentration at these two sites.

With reference to Site D, temperature is surely a driving factor in the volatilization of NH_3(g) from fertilizer in agricultural soil. That is likely the reason the enhancement of fertilizer application at the end of June 2018 for the summer crop and February 2019 for the spring crop corresponded with the highest and the second-highest concentration of NH_3(g) in summer and spring, respectively. The non-application of fertilizer in autumn and winter could explain the low level of NH_3(g) concentrations during these seasons. Thus, the use of fertilizer for agricultural crops combined with the change in ambient temperature appeared to govern the variation in NH_3(g) concentration in the suburban area of Hanoi. Regarding Site B, the concentration in summer was significantly higher than those in other seasons. The high temperature in summer strengthens the biological decomposition of organic substances in the wastewater of the polluted river, which increases the release of NH_3(g) from the river body into the atmosphere more than in other seasons with lower temperatures. Interestingly, apart from the ambient temperature, a statistically significant correlation between NH_3(g) concentration and relative humidity (RH) was also found at sites B ($r = -0.547$, $p < 0.001$) and D ($r = -0.634$, $p < 0.001$).

Table 3.5. Correlation coefficients between Daily and Weekly concentration and meteorological factors.

	Weekly concentration (Site A)		Daily concentration							
			Site A		Site B		Site C		Site D	
	Pearson's R	*p-value*	Pearson's R	*p-value*	Pearson's R	*p-value*	Pearson's R	*p-value*	Pearson's R	*p-value*
Temperature [^{o}C]	-0.0258	0.4301	-0.0539	0.3790	0.5553	**0.0002**	0.0564	0.3735	0.4702	**0.0020**
Relative humidity [%]	0.2119	0.0719	0.11185	0.2486	-0.5472	**0.0003**	-0.1007	0.2822	-0.6339	**0.0000**

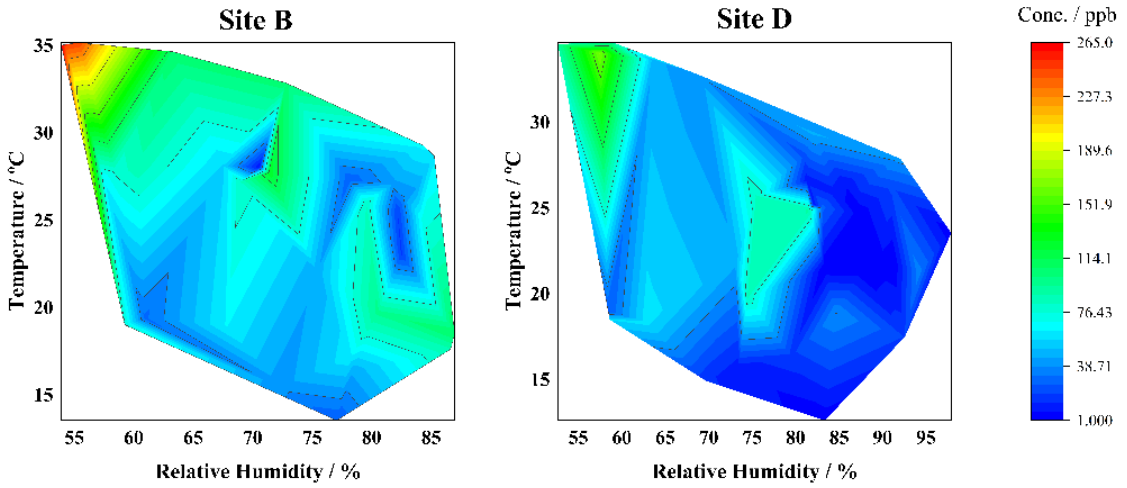

Figure 3.4. Relative humidity and temperature dependence of NH_3(g) concentration at sites B and D in Hanoi.

The equilibrium shift between NH_3(g) and NH_4NO_3 would be a process involved in this phenomenon. The study area in this research had an RH ranging from around 53 to 98%, which was higher than the estimated deliquescence relative humidity (DRH) of NH_4NO_3 (i.e., 62% at 298 K) during most of the sampling period. This condition was thermodynamically favorable for the formation of NH_4NO_3 due to the uptake of water when HNO_3 and NH_3 aggregated (Kobara et al., 2007; Behera et al., 2013), which would be responsible for the reduction of NH_3(g) in the atmosphere. Figure 3.4 shows the impact of RH and temperature on the NH_3(g) concentration at Site B and Site D. At both sites, the high NH_3(g) concentration existed under the condition of a high temperature range (30–35 ^oC) and low humidity range (55–60%), which is below the DRH of NH_4NO_3. Hence, it seems that the RH can also influence the NH_3(g) concentration at sites B and D.

It is quite clear that the statistical significance in the correlation of temperature and relative humidity with concentration appears at sites B and D rather than sites A and C. Site C, which is representative of traffic emissions, could be more sensitive to the driving conditions (Section 3.3.2) than the effect of temperature and relative humidity. Site A is representative of a typical urban area, which is under the total influence of a complex interplay between

atmospheric chemical processes and various sources instead of a particular one, so these meteorological factors can rarely govern the change in concentration level at this site. Besides temperature and RH, wind direction also is one of important parameters to the fate of NH_3(g) at local scale. The distinctly high concentration in the summer sampling period at Site B could result in unexpectedly high concentrations at sites A and C because of the local transportation of NH_3(g) from the intense emission source of the polluted river under the effect of wind direction.

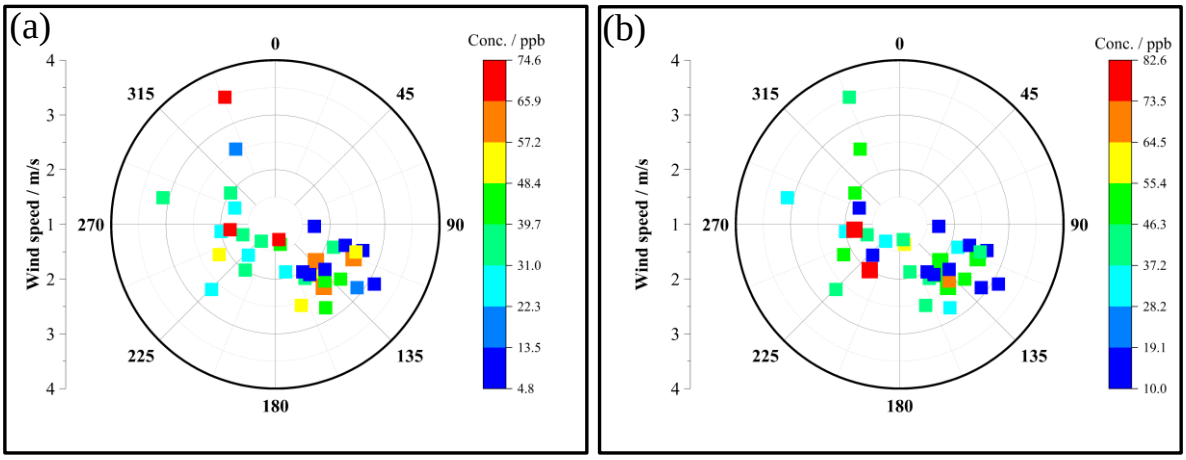

Figure 3.5. The dependence of NH_3(g) concentration on wind speed (WS) and wind direction (WD) at (a) Site A, and (b) Site C in the urban area of Hanoi. Radial data are WS [m/s]. Angular data are WD [o]. The colors denote the NH_3(g) concentrations [ppb].

Regarding Site A, the last three days of summer experienced moderately high concentrations (ca. 63 ppb) (Fig. 3.2(a)). The bivariate polar plot of NH_3(g) concentration at Site A (Fig. 3.5(a)) shows that these moderately high concentrations are mainly attributed to south east (i.e., east-southeast (ESE), southeast (SE), and south-southeast (SSE)) sector. Taking the situation of the river (Fig. 3.6) into account, the wind from the south east sector would likely bring the NH_3(g) from the river to Site A as a downwind site.

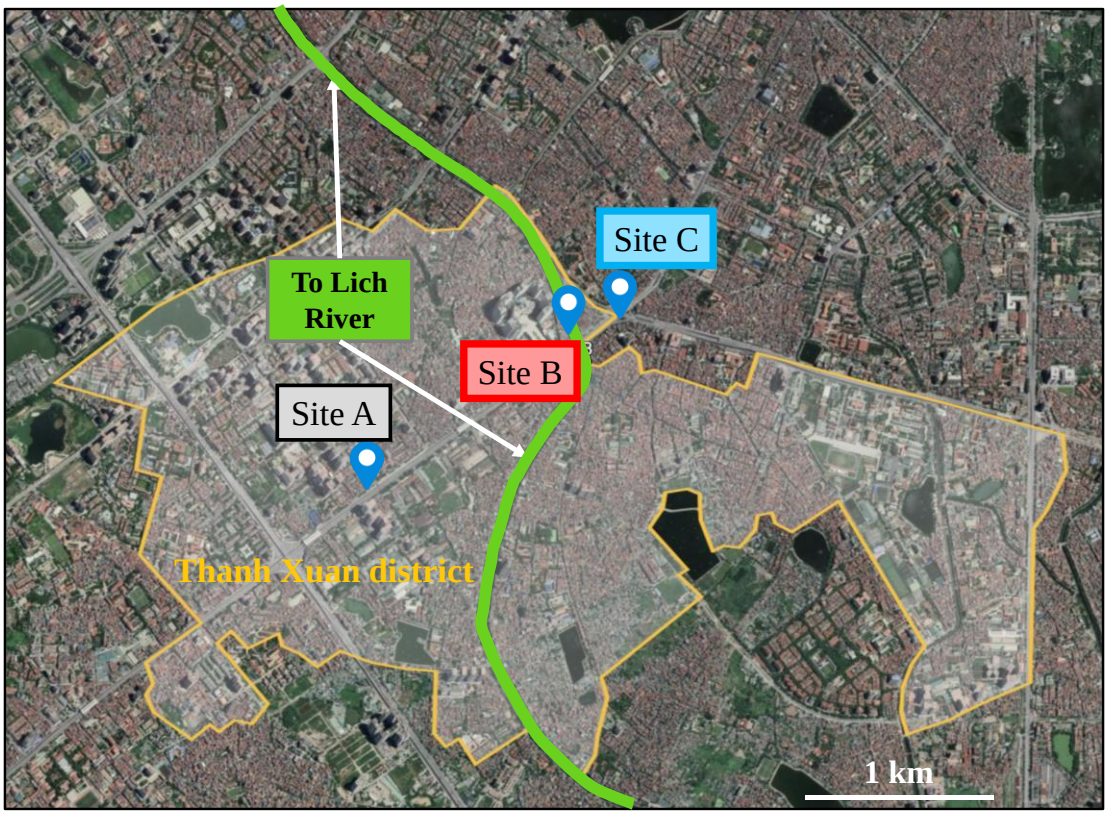

Figure 3.6. Relative position of survey sites with To Lich River in urban area of Hanoi.

In terms of Site C, the first day of summer had the highest concentration 82.6 ppb (Fig. 3.2(a)), which is attributed to southwest (SW) sector (Fig. 3.5(b)). Site C locates in downwind position with the river, thus could be affected by the transportation of NH_3(g) from the river by the wind from the SW. Therefore, particularly in an urban area, intense local emissions from a polluted river in the summer could have a strong influence on the rise in the concentration of the surrounding area under the effect of the wind direction.

Besides the analysis of the impact of local wind direction to the delivery of NH_3(g) emitted from a particular source to surrounding area, backward trajectory was also taken into account to analyze the effect of transboundary transportation (i.e., regional scale) on NH_3(g) concentration in Hanoi (Section S3). Nevertheless, the regional transboundary transportation of air masses seems to have no effect on the change of NH_3(g) concentration.

Seasonal variation based on weekly sampling at Site A

Figure 3.7 shows the seasonal mean of weekly concentrations collected at Site A, the abnormally high values due to human-induced errors were replaced by the mean of the corresponding season in the calculation. Unlike the seasonal pattern of daily sampling basis, the seasonal variation in weekly concentrations collected at Site A (i.e., typical downtown area) (Fig. 3.7), which is representative for the temporal variation of the urban area throughout the entire year, shows that winter and autumn had the highest concentrations of 37.5±14.3 and 37.2±4.0 ppb, respectively, followed by summer (30.8±9.3 ppb), and spring saw the lowest concentration of 23.3±8.0 ppb. The NH_3(g) concentration on the weekly basis was independent of temperature; r = -0.026, $p > 0.05$ (Table 3.5).

The phenomenon of higher concentrations in colder seasons has hardly been seen according to conventional wisdom and the results of most previous studies, in which a seasonal peak was regularly reported in summer or spring (Lee et al., 1999; Chang et al., 2016; Wu et al., 2018). Nevertheless, more recently, this seasonal variation pattern has also been recognized in non-agriculturally based sites in Kobe and Kitakyushu, Japan (Nguyen et al., 2021), where, in the cold season, the production of more NH_3(g) under the fuel-rich combustion condition of engines in order to reach and maintain an optimal operating temperature is partially responsible for this situation. Meng et al. (2011) and Zhou et al. (2019) emphasized traffic as a significant emission source of NH_3 in winter in the urban areas of Beijing and New York State, respectively. Indeed, the drastic increase in traffic density in February caused by the surging travel demand during the traditional Tet holiday could be the cause of the highest concentration in February, 49.4±7.4 ppb (Fig. 3.7).

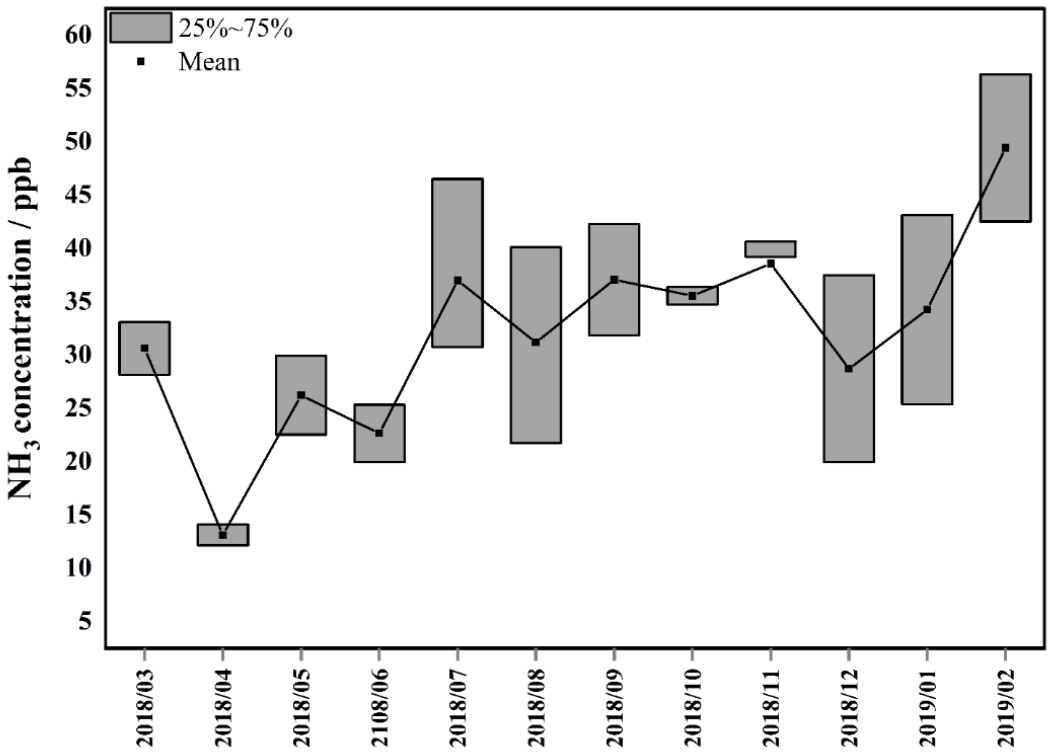

Figure 3.7. Monthly variation in NH_3(g) concentration of weekly sampling basis at Site A in Hanoi.

Thus, in downtown Hanoi, basically, the NH_3(g) concentration is higher in colder seasons than in warmer seasons, which implies that vehicular emissions would be an important contributor to NH_3(g) emissions.

3.4. Conclusions

The NH_3(g) concentrations were measured using a passive sampling method in four source-specific locations which focus on the impact of typical downtown, intersection, polluted river, and rural areas of Hanoi, Vietnam, from March 2018 to February 2019 on a daily and weekly basis.

The NH_3(g) concentrations were discussed from the viewpoint of spatial distribution. A distinctly high concentration (79.8±61.2 ppb) from a polluted river was indicated as an important source unheard of in an urban area. The concentrations at the intersection (Site C), downtown (Site A), and rural area (Site D) experienced a much lower level than that of the

polluted river (Site B). In which, the concentration at Site C (38.6±18.8 ppb) was slightly higher than that of Site A (36.5±20.0 ppb), followed by the lowest concentration (35.6±36.0 ppb) in the rural area (Site D).

In addition, the seasonal variation in NH_3(g) concentration, along with the effect of meteorological factors, was analyzed. Basically, in downtown Hanoi, the NH_3(g) concentration was higher in cooler seasons (i.e., autumn and winter) than in warmer seasons because of the enhanced emission of NH_3(g) from vehicles in lower temperature conditions. Thus, vehicular emissions are suggested to be a primary contributor to NH_3(g) emissions in the urban Hanoi area. In the rural area, summer is the season with the highest values, followed by spring. The application of fertilizer to agricultural crops is suggested to be a major emission source of NH_3(g) at this site, which is sensitive to the change in meteorological conditions in terms of temperature and relative humidity. The polluted river, even though located in an urban area, had the highest concentration in summer. Like the rural area, the change in temperature and relative humidity appears to govern the variation in NH_3(g) concentration by affecting the volatilization of NH_3(g) from the wastewater in the river. Furthermore, the intense emitted NH_3(g) from the polluted river in summer would, in particular, have a strong local influence on the increase in NH_3(g) concentration of the surrounding area from the impact of local wind as a transporting factor.

References

Aneja, V.P., Bunton, B., Walker, J.T., Malik, B.P. (2001). Measurement and analysis of atmospheric ammonia emissions from anaerobic lagoons. *Atmospheric Environment* **35**: 1949–1958. https://doi.org/10.1016/S1352-2310(00)00547-1.

Bajwa, K.S., Aneja, V.P., Pal Arya, S. (2006). Measurement and estimation of ammonia emissions from lagoon–atmosphere interface using a coupled mass transfer and chemical reactions model, and an equilibrium model. *Atmospheric Environment* **40**: 275–286. https://doi.org/10.1016/J.ATMOSENV.2005.12.076.

Behera, S.N., Sharma, M., Aneja, V.P., Balasubramanian, R. (2013). Ammonia in the atmosphere: A review on emission sources, atmospheric chemistry and deposition on terrestrial bodies. *Environmental Science and Pollution Research* **20**: 8092–8131. https://doi.org/10.1007/s11356-013-2051-9.

Bouwman, A.F., Lee, D.S., Asman, W.A.H., Dentener, F.J., Hoek, V.D.K.W., Olivier, J.G. (1997). A global high-resolution emission inventory for ammonia. *Global Biogeochemical Cycles* **11**: 561-587. https://doi.org/10.1029/97GB02266.

Chang, Y., Zou, Z., Deng, C., Huang, K., Collett, J. L., Lin, J., Zhuang, G. (2016). The importance of vehicle emissions as a source of atmospheric ammonia in the megacity of Shanghai. *Atmospheric Chemistry and Physics* **16(5)**: 3577–3594. https://doi.org/10.5194/acp-16-3577-2016.

Cohen, D.D., Crawford, J., Stelcer, E., Bac, V.T. (2010). Characterisation and source apportionment of fine particulate sources at Hanoi from 2001 to 2008. *Atmospheric Environment* **44**: 320–328. https://doi.org/10.1016/j.atmosenv.2009.10.037.

Dai, X.R., Saha, C.K., Ni, J.Q., Heber, A.J., Blanes-Vidal, V., Dunn, J.L. (2015). Characteristics of pollutant gas releases from swine, dairy, beef, and layer manure, and

municipal wastewater. *Water Research* **76**: 110–119. https://doi.org/10.1016/j.watres.2015.02.050.

Department of Transport, 2017. Hanoi Portal. https://hanoi.gov.vn/tintuc_sukien/-/hn/ZVOm7e3VDMRM/3/2798413/40/40/16.html;jsessionid=KuWRCqBcBnxV7SWBVBs1t-Fa.app2?doAsUserId=_viewTinTucId%3D122202 (last access: 2021/10/27).

Dinh Dap, N. (2019). Impacts of wastewater from main factories on water quality of Tolich river, Hanoi. *E3S Web Conference* **91**: 1–8. https://doi.org/10.1051/e3sconf/20199104001.

General Statistics Office, 2016. Area, population and population density. https://www.gso.gov.vn/px-web-2/?pxid=V0201&theme=D%C3%A2n%20s%E1%BB%91%20v%C3%A0%20lao%20%C4%91%E1%BB%99ng (last access: 2021/08/24).

Ha, T.D., Hung, L.V., Duc, T., Hai, M., Anh, T.T. (2020). Forecast of water quality of Tolich river based on scenarios of Hanoi sewerage planning by using model QUAL2K. *Vietnam Journal of Science and Technology* **58**: 75–83. https://doi.org/10.15625/2525-2518/58/3A/14269.

Heeb, N.V., Forss, A.-M., Brühlmann, S., Lüscher, R., Saxer, C.J., Hug, P. (2006). Three-way catalyst-induced formation of ammonia- velocity- and acceleration-dependent emission factors. *Atmospheric Environment* **40 (31)**: 5986–5997. https://doi.org/10.1016/j.atmosenv.2005.12.035.

Hien, P.D., Bac, V.T., Tham, H.C., Nhan, D.D., Vinh, L.D. (2002). Influence of meteorological conditions on $PM_{2.5}$ and $PM_{2.5-10}$ concentrations during the monsoon season in Hanoi, Vietnam. *Atmospheric Environment* **36**: 3473–3484. https://doi.org/10.1016/S1352-2310(02)00295-9.

Hien, P.D., Hangartner, M., Fabian, S., Tan, P.M. (2014). Concentrations of NO_2, SO_2, and benzene across Hanoi measured by passive diffusion samplers. *Atmospheric Environment* **88**: 66–73. https://doi.org/10.1016/j.atmosenv.2014.01.036.

Hien, P.D., Men, N.T., Tan, P.M., Hangartner, M. (2020). Impact of urban expansion on the air pollution landscape: A case study of Hanoi, Vietnam. *Science of the Total Environment* **702**, 134635. https://doi.org/10.1016/j.scitotenv.2019.134635.

Hopke, P.K., Cohen, D.D., Begum, B.A., Biswas, S.K., Ni, B., Pandit, G.G., Santoso, M., Chung, Y.S., Davy, P., Markwitz, A., Waheed, S., Siddique, N., Santos, F.L., Pabroa, P.C.B., Seneviratne, M.C.S., Wimolwattanapun, W., Bunprapob, S., Vuong, T.B., Duy Hien, P., Markowicz, A. (2008). Urban air quality in the Asian region. *Science of the Total Environment* **404**: 103–112. https://doi.org/10.1016/j.scitotenv.2008.05.039.

Huai, T., Durbin, T.D., Miller, J.W., Pisano, J.T., Sauer, C.G., Rhee, S.H., Norbeck, J.M. (2003). Investigation of NH_3 Emissions from New Technology Vehicles as a Function of Vehicle Operating Conditions. *Environmental Science and Technology* **37**: 4841–4847. https://doi.org/10.1021/es030403+.

Kim Oanh, N.T., Upadhyay, N., Zhuang, Y.-H., Hao, Z.-P., Murthy, D.V.S., Lestari, P., Villarin, J.T., Chengchua, K., Co, H.X., Dung, N.T., Lindgren, E.S. (2006). Particulate air pollution in six Asian cities: Spatial and temporal distributions, and associated sources. *Atmospheric Environment* **40**: 3367–3380. https://doi.org/10.1016/J.ATMOSENV.2006.01.050.

Kobara, H., Takeuchi, K., Ibusuki, T. (2007). Effect of Relative Humidity on Aerosol Generation through Experiments at Low Concentrations of Gaseous Nitric Acid and Ammonia. *Aerosol and Air Quality Research* **7(2)**: 193-204. https://doi.org/10.4209/aaqr.2006.10.0023.

Lee, H. S., Kang, C.-M., Kang, B.-W. and Kim, H.-K. (1999). Seasonal variations of acidic air pollutants in Seoul, South Korea. *Atmospheric Environment* **33(19)**: 3143–3152. https://doi.org/10.1016/S1352-2310(98)00382-3.

Livingston, C., Rieger, P., Winer, A. (2009). Ammonia emissions from a representative in-use fleet of light and medium-duty vehicles in the California South Coast Air Basin. *Atmospheric Environment* **43**: 3326–3333. https://doi.org/10.1016/j.atmosenv.2009.04.009.

Meng, Z. Y., Lin, W. L., Jiang, X. M., Yan, P., Wang, Y., Zhang, Y. M., Jia, X. F., Yu, X. L. (2011). Characteristics of atmospheric ammonia over Beijing, China. *Atmospheric Chemistry and Physics* **11(12)**: 6139-6151. https://doi.org/10.5194/acp-11-6139-2011.

Ministry of Natural Resources and Environment, 2014. National Environmental Status Report 2013: Atmospheric environment (In Vietnamese).

Ministry of Natural Resources and Environment, 2016. National Environmental Status Report 2011 – 2015. Chapter 5: Atmospheric Environment, 101 – 116 (In Vietnamese).

Ministry of Natural Resources and Environment, 2017. National Environmental Status Report 2016. Chapter 2: Atmospheric Environment, 25 – 45 (In Vietnamese).

Mohammed-Nour, A., Al-Sewailem, M., El-Naggar, A.H. (2019). The influence of alkalization and temperature on Ammonia recovery from cow manure and the chemical properties of the effluents. *Sustainability* **11**: 2441. https://doi.org/10.3390/su11082441.

Nguyen, D. V., Sato, H., Hamada, H., Yamaguchi, S., Hiraki, T., Nakatsubo, R., Murano, K., Aikawa, M. (2021). Symbolic seasonal variation newly found in atmospheric ammonia concentration in urban area of Japan. *Atmospheric Environment* **244**: 117943. https://doi.org/10.1016/j.atmosenv.2020.117943.

Ni, J.-Q., Heber, A.J., Sutton, A.L., Kelly, D.T. (2009). Mechanisms of gas releases from swine wastes. *Transaction of the ASABE* **52(6)**, 2013-2025. http://dx.doi.org/10.13031/2013.29203.

Sakamoto, Y., Shoji, K., Bui, M.T., Phạm, T.H., Vu, T.A., Ly, B.T., Kajii, Y. (2018). Air quality study in Hanoi, Vietnam in 2015–2016 based on a one-year observation of NO_x, O_3, CO and a one-week observation of VOCs. *Atmospheric Pollution Research* **9**: 544–551. https://doi.org/10.1016/j.apr.2017.12.001.

Thom, D.T. (2013). Nghiên cứu sự biến động đất nông nghiệp do ảnh hưởng của quá trình công nghiệp hóa và đô thị hóa huyện Sóc Sơn, thành phố Hà Nội.

Wu, S.-P., Dai, L.-H., Wei, Y., Zhu, H., Zhang, Y.-J., Schwab, J. J., Yuan, C.-S. (2018). Atmospheric ammonia measurements along the coastal lines of Southeastern China: Implications for inorganic nitrogen deposition to coastal waters. *Atmospheric Environment* **177**: 1-11. https://doi.org/10.1016/j.atmosenv.2017.12.040.

Yao, X., Hu, Q., Zhang, L., Evans, G.J., Godri, K.J., Ng, A.C. (2013). Is vehicular emission a significant contributor to ammonia in the urban atmosphere? *Atmospheric Environment* **80**: 499–506. https://doi.org/10.1016/j.atmosenv.2013.08.028.

Zheng, J.Y., Yin, S.S., Kang, D.W., Che, W.W., Zhong, L.J. (2012). Development and uncertainty analysis of a high-resolution NH3 emissions inventory and its implications with precipitation over the Pearl River Delta region, China. *Atmospheric Chemistry and Physics* **12**: 7041–7058. https://doi.org/10.5194/acp-12-7041-2012.

Zhou, C., Zhou, H., Holsen, T. M., Hopke, P. K., Edgerton, E. S., Schwab, J. J. (2019). Ambient Ammonia Concentrations Across New York State. *Journal of Geophysical Research: Atmospheres* **124(14)**: 8287-8302. https://doi.org/10.1029/2019JD030380.

Chapter 4. Summary and future prospect

4.1. Summary

In summary, the NH_3(g) concentrations were measured using the passive sampling method for one year in a source-specific campaign in Japan and Vietnam with the aim of providing the comprehensive insight into the characteristics and behaviors of NH_3(g) in the atmosphere, then pointing out the differences between a developed and developing country. Based on the results of this study, the thesis has four main conclusions as the following:

Conclusion 1: The disparity between NH_3(g) concentration in Japan and Vietnam

There was a huge disparity between the NH_3(g) concentration in Japan and Vietnam, in which, the NH_3(g) concentration in Japan is much lower than that in Vietnam. In detail, among the survey sites in Japan, the annual mean NH_3(g) concentration was 2.08±0.9 ppb (range from 0 ppb to around 5 ppb) in Kobe, and 4.28±1.7 ppb in Kitakyushu (range from 0 to 8.94 ppb); while the annual average concentration in Hanoi, Vietnam was around 32.3±11.2 ppb (range from 6.6 to 59.8 ppb).

Conclusion 2: Spatial distribution and corresponding emission sources

In Kobe, Japan, the NH_3(g) concentration was the highest (3.10 ppb) at the site where the contribution of agriculture was noticeably large in the NH_3 inventory regardless of any controlling factors, followed by commercial and residential areas (ca. 2.00 ppb), while it was the lowest at the mountainous site with high elevation (0.91 ppb). Among multiple controlling factors (i.e., site situation, land use around the sites, meteorological condition, and NH_3 inventory), which were mutually related and contributed to the spatial distribution, the proportion of Human&Pet to the NH_3 inventory could be the most effective parameter for potentially accounting for the NH_3(g) concentration in urban area.

In Vietnam, a distinctly high concentration (79.8±61.2 ppb) was indicated at the polluted river, an important source unheard of in urban areas, followed by the crossroad (38.6±18.8 ppb) and the downtown (36.5±20.0 ppb); the lowest concentration (35.6±36.0 ppb) was observed in the rural area. The concentration was highly affected by the nearby emission sources.

While the major contribution of agricultural emissions to NH_3(g) concentration was seen in Japan, the proportion of agricultural emissions in Vietnam was overwhelmed by other emission sources in urban area, suggesting that the urban area was seriously suffered from NH_3(g) pollution, which is much more harmful to residents' health as concentrated population density in urban area.

Conclusion 3: Temporal variation

In both urban areas of Kobe and Kitakyushu, Japan, the NH_3(g) concentration indicated lower level in the summer than those in other seasons and experienced higher concentration in colder period, which was newly found compared with the conventional wisdom and results in former studies. Acid-base balance in the atmospheric reaction and vehicular emission were mutually related and presumably responsible for the seasonality of higher in the colder seasons and lower in the warmer season.

The phenomenon of higher concentration in colder seasons was also observed in the downtown of Hanoi, Vietnam, also implying the major impact of vehicular emission on the rise of NH_3(g) in urban area.

Conclusion 4: Effect of meteorological parameters

In Hanoi, particularly, temperature and relative humidity strongly govern NH_3(g) concentration level at polluted river and rural area due to the strong impact of these

meteorological factors on the volatilization of NH_3(g) from wastewater and agriculture, respectively, causes the highest concentration in summer at these sites. The high concentration at this site was transferred to surrounding area by local wind, causing the unexpectedly high concentration at the downtown in Hanoi in summer.

Furthermore, in Kobe, the local wind was also supposed to have significant impact to transfers NH_3(g) intensely emitted from a particular source to the surrounding areas, causing the homogenous characteristic (i.e., less disparity among sites) of NH_3(g) in entire area.

The transboundary transportation of air parcels seems to have no effect on the change of NH_3(g) concentration (Section S3).

4.2.Novelty/ significance

The data on NH_3(g) has been limitedly reported, so the data collected in this field-experimental campaign would provide a precious value to the data base on NH_3(g) concentration worldwide, especially, this is the first time, a study about NH_3(g) in Hanoi, Vietnam was conducted.

The symbolic seasonal variation was newly found in urban area of both Vietnam and Japan, in which, the cooler seasons witnessed higher concentrations, mostly implying the increasingly severe contribution of vehicular emissions in urban area.

The intense emission from polluted river was unprecedentedly reported in Hanoi, Vietnam, which might be applicable to other developing countries when the drainage system has not yet been fully solved. The research about NH_3(g) emission from wastewater body and/or wastewater treatment plants also need more attention from scientists' community as their huge impact on the urban atmosphere.

The reported data in this thesis are valuable for not only the environmental scientist's community but also the governmental levels to be aware of the pollution situation of NH_3(g)

in the urban area, then come up with appropriate solutions.

4.3. Future prospect

In this present study, the NH_3(g) concentration was solely measured. The NH_3(g) concentration is not only driven by the NH_3 emission and impact of various controlling factors but atmospheric chemical reactions are also an important factor. Thus, the homogenous analysis of the influence of other gases such as HNO_3(g), on the change of NH_3(g) concentration, is essential to get greater insight into the behavior of NH_3(g), and the interaction between NH_3(g) and other atmospheric species.

What is more, the NH_3(g) concentration in urban area of Hanoi, Vietnam was determined much higher than that in Japan (i.e., around 10 times), which might raise a question of whether this high level of NH_3(g) concentration, itself, has serious effect on the human health. Thus, beside the indirect impact on the human health via the formation of inorganic aerosol, the assessment of direct impact of NH_3(g) on the human health should be investigated carefully in further studies.

Publication list

Nguyen, D. V., Sato, H., Hamada, H., Yamaguchi, S., Hiraki, T., Nakatsubo, R., Murano, K., Aikawa, M., 2021. Symbolic seasonal variation newly found in atmospheric ammonia concentration in urban area of Japan. Atmospheric Environment **244**: 117943. https://doi.org/10.1016/j.atmosenv.2020.117943

Van Nguyen, D., Nguyen, L.K., Tran, D.A., Duong, M.H., Nguyen, H.T., Aikawa, M., 2022. Seasonal variation of NH_3 concentration and its controlling factors in Hanoi, Vietnam, depending on the site classification. International Journal of Environmental Science and Technology. https://doi.org/10.1007/s13762-022-04567-0

Acknowledgments

In my adventure of chasing a new horizon of knowledge, this journey has bestowed on me the privilege to meet and learn from many wonderful people from all walks of life. I wish to fully appreciate all their help, but for limited space, particularly name a few of them.

Firstly, the most important person that I would like to show my deepest appreciation of his all kindly, conscientious support, guidance, instruction, encouragement, and caring during my entire 5-year journey of MS-Ph.D. studying at Graduate School of Environmental Systems, The University of Kitakyushu (UKK) is my supervisor, Professor Masahide AIKAWA. His greatest patience and respect toward student's idea provide me a freedom to set foot on new approach in doing research. His supervision with full of wisdom did show me precious lessons. 5-year working with him had equipped me with scientist-like mindset, which is proved much of useful even in the case of enrolling into industry. Working with him, I have not only attempted to be extremely careful at work, but also matured in many other aspects, especially "always stand on others' positions" is what I have trained to execute for better life of myself and others.

I also thank the members of my thesis examining committee, Prof. Hitoshi Ohya, Prof. Takaaki Kato, and Prof. Takeshi Nishida, who spent precious time evaluating and giving comments to my thesis.

I would like to express my sincere gratitude to Prof. Nguyen Thi Ha, Faculty of Environment, VNU University of Science for her support in conducting sampling campaign in Vietnam.

During my studying and research at UKK, I have also received a number of valuable advice and help from other laboratory members: Dr. Xi Zhang - senior, I have learnt from her so much; Ms. Peng Yuan, for her always beside for 5 years; my Vietnamese friends Nguyen

Tran Dung and Tran Anh Duy, we all have nice time together. My special thank goes to Nguyen Khanh Linh, who is not only my colleague, but also one of my close friends, we have experienced the whole journey together.

In retrospect, I am indebted to all lab's members, who come-and-go but memories have stayed: Ms. Momoko Abe, Mr. Sho Oniwa for their sharing not only knowledge but also Japanese understanding; other members in our laboratory: Mr. Taiki Hiramoto, Mr. Shota Ono, Mr. Takuya Murakami, Mr. Yuga Tamura, Mr. Shota Tominaga, Ms. Miu Suzuki, Mr. Akito Nakazono, Mr. Takahiro Shimozono, Ms. Akari Ishida, Ms. Nami Takata, Mr. Taisei Kamo, Ms. Mana Kondo, Ms. Ayane Aoyama, Mr. Yuta Iwamoto, Mr. Tsuyoshi Ogami, Mr. Hayato Imazu, Ms. Ayano Tomura for their kindly support and enjoyable atmosphere.

I would like to show my attitude to all researchers in Tobata and Kobe, Japan, and Hanoi, Vietnam for their cooperation and assistance in taking sampling during the time. Without their generous support, this thesis would be impossible.

Last but not least, I am wholeheartedly thankful to my dear family, especially, my father Nguyen Van Nguyen, my mother Phung Thi Tuyet, my wife Ton Thi Minh Thu and my son Nguyen Ton Lam, who are always by my side, encourage me in both studying and life. I am fortunately blessed with your love and belief.

Thanks for everything and everyone, which come and go, my life cannot be fulfilled without you all.

Thank you! / ありがとうございました！/ Cảm ơn!

Nguyen Van Duy

Supplementary Information

S1. Meteorological parameters assess to ISD

For the analysis of meteorological parameter in this study, the high time-resolution data is essential. In order to access the Global Hourly data from the Integrated Survey Database (ISD) of the National Centers for Environmental Information, US National Oceanic and Atmospheric Administration (NOAA), the NCEI Data Access app only provide hourly compiled into a single common ASCII format and common data model.

Thus, using R program and the "*worldmet*" package helps to import those data with ease, then "*rio*" package would help to convert the original files into csv file, which might reduce a bunch of work in data treatment.

S2. Nonparametric wind regression

Nonparametric wind regression (NWR) is a source-to-receptor source apportionment model that has been developed by Environmental Protection Agency (EPA). The model uses nonparametric kernel smoothing methods to apportion the observed average concentration of a pollutant to sectors defined by ranges of wind direction and speed to identify and quantify the impact of possible source regions of pollutants as defined by wind direction sectors (Henry et al., 2009; Donnelly et al., 2011; Pancras et al., 2011).

The NH_3(g) concentration C at a receptor is expressed as the function of wind direction θ and wind speed u. The average concentration of NH_3(g) for a particular wind direction and speed pair (θ, u) is calculated as a weighted average of the concentration data in a window around (θ, u) represented by smoothing parameters σ_1 and σ_2 using a weighting function $K(\theta, u, \sigma_1, \sigma_2) = K(\theta, \sigma_1)(u, \sigma_2)$, also known as the kernel function.

The expected value of C given θ and u is estimated by

$$1.\quad E(C|\theta,u)=\frac{\sum_{i=1}^{N}K\left(\frac{(\theta-W_i)}{\sigma_1}\right)\left(\frac{(u-U_i)}{\sigma_2}\right)C_i}{\sum_{i=1}^{N}K\left(\frac{(\theta-W_i)}{\sigma_1}\right)\left(\frac{(u-U_i)}{\sigma_2}\right)} \qquad (1)$$

Where Ci, Wi and Ui are the observed concentration of NH_3(g), wind direction and speed, respectively, for the i^{th} observation in a time period starting at time ti, N is the total number of observations.

The R program, downloaded from https://www.r-project.org, and the "*openair*" package (Carslaw, 2019) were employed to calculate and plot the polar concentrations. In the approach adopted in *openair*, Gaussian smoothing method are used for both wind speed and wind direction. The kernel function used in this work is the Gaussian kernel given by

$$2.\quad K(x)=(2\pi)^{-\frac{1}{2}}\exp(-0.5x^2),-\infty<x<\infty \qquad (2)$$

The width (bandwidth - σ) of the Gaussian kernels is controlled by the options wind direction spread and wind speed spread, in which, wind direction spread is the value of σ1 used for Gaussian kernel weighting of wind direction and wind speed spread is the value of σ2 used for Gaussian kernel weighting of wind speed. In this study, the σ1 and σ2 values were set at default of 4 directions and 0.5 m/s, respectively.

Fig. S1 shows the bivariate polar plot of sites A and C in terms of nonparametric regression application.

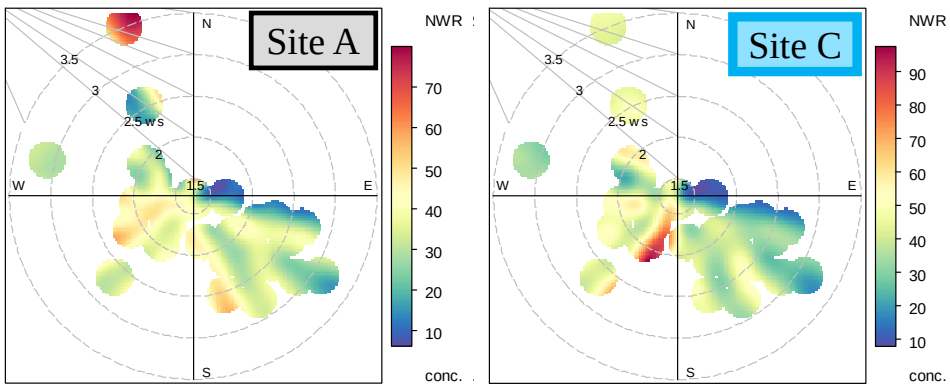

Figure S1. Bivariate polar plot of non-parametric wind regression of sites A, and C.

Furthermore, the map polar plot might be much of beneficial to provide a more interactive visualization to the polar plot in the corresponding situation in the leaflet map (the following attached webpage file).

O_polarmap.html

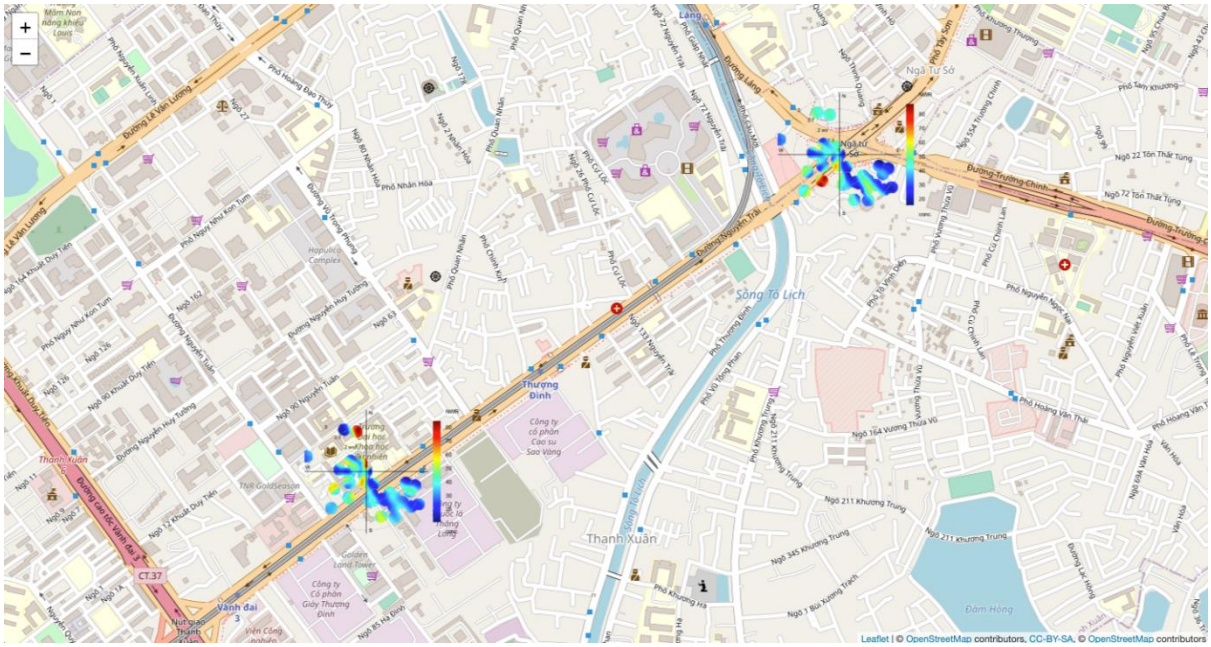

Figure S2. Bivariate polar plot of sites A and C in the urban map of Hanoi.

Because of the small size of the data set in this study, the application of kernel smoothing method might cause the confusion to determine the sector of moderate concentration. However, this approach would be much more beneficial with a large size database in further studies.

S3. Trajectory analysis

NH_3(g) has a very short atmospheric lifetime of only a day or less because of rapid deposition and particle uptake (Zhu et al., 2015; Nair and Yu, 2020). Therefore, the 24-h backward trajectories (Fig. S3) were calculated with a starting height of 1000 m above ground level and starting point of Site A using HYSPLIT 5.0 model obtained from the NOAA Air

Resources Laboratory (https://www.ready.noaa.gov/HYSPLIT.php). The trajectory calculations were done for each hour (i.e., one hour interval) of each day during entire Daily sampling period.

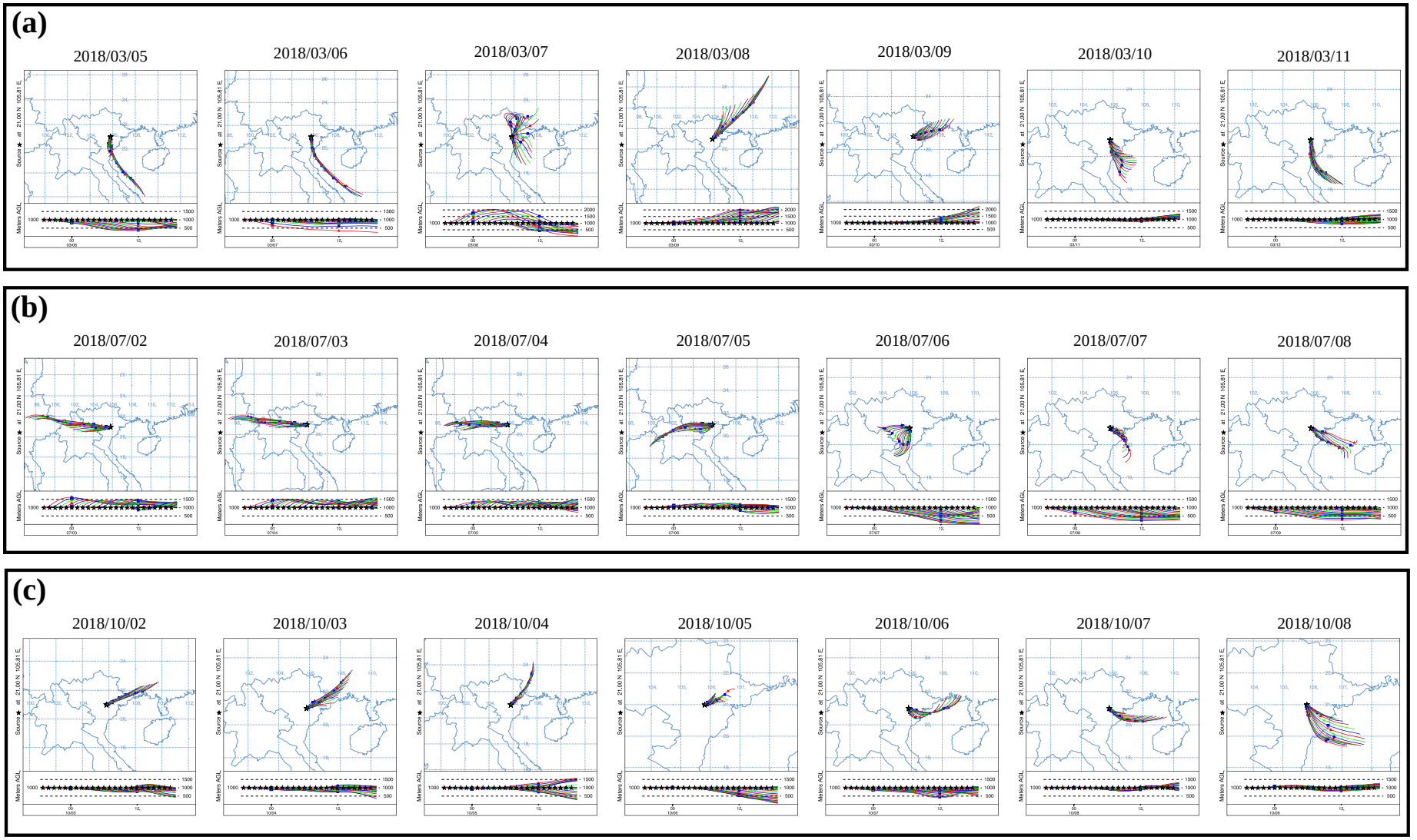
(a)
2018/03/05
2018/03/06
2018/03/07
2018/03/08
2018/03/09
2018/03/10
2018/03/11
(b)
2018/07/02
2018/07/03
2018/07/04
2018/07/05
2018/07/06
2018/07/07
2018/07/08
(c)
2018/10/02
2018/10/03
2018/10/04
2018/10/05
2018/10/06
2018/10/07
2018/10/08

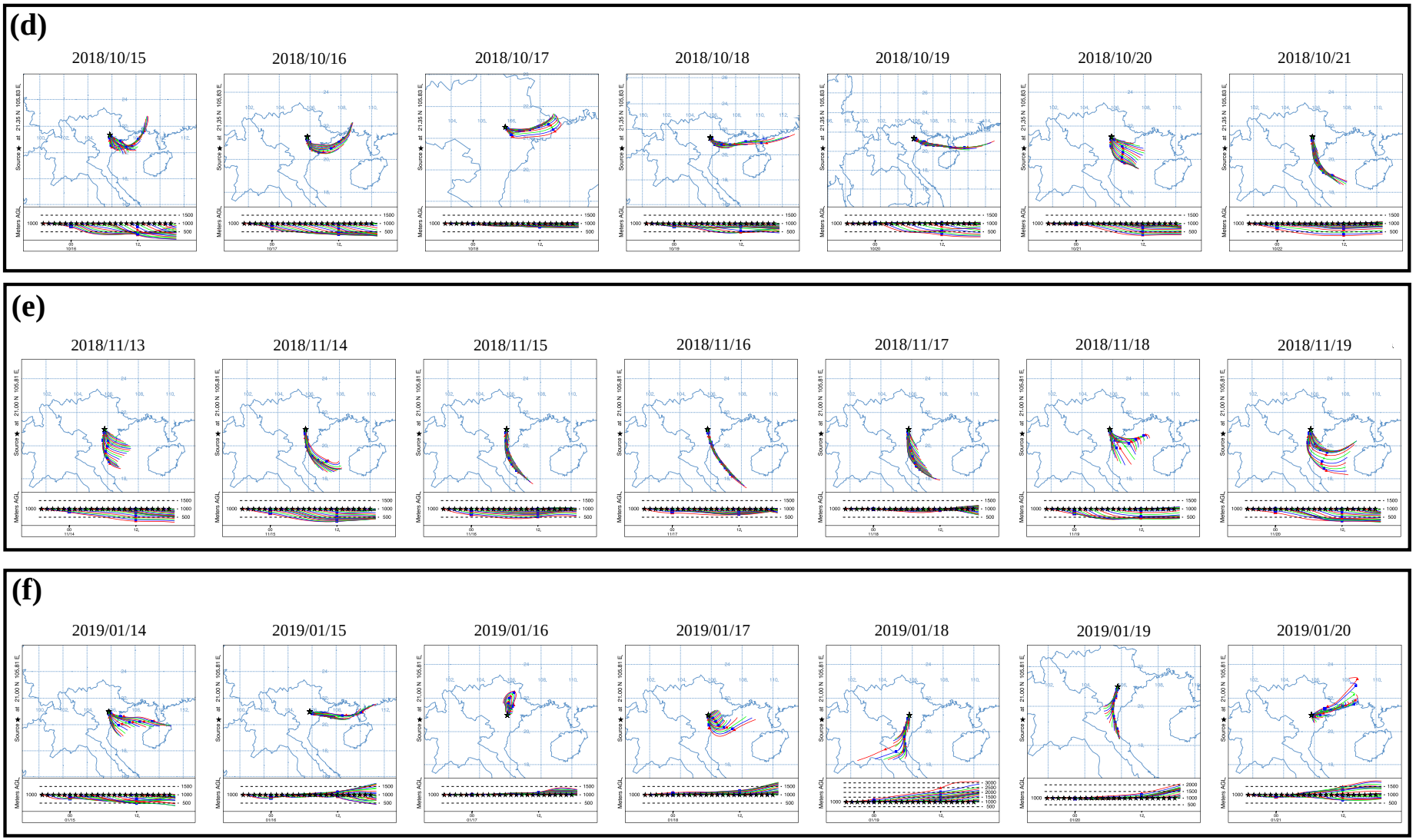

Figure S3. The backward trajectories in daily sampling basis in Hanoi: spring (a), summer (b), transition 1 (c), transition 2 (d), autumn (d), and winter (e).

In spring, the trajectories transported in near surface (≤ 1000 m) were highly corresponding with the higher concentration, while those from higher altitudes (2000 m) were corresponding with lower concentration on March 7^{th} and 8^{th}. On the contrary, in summer, the trajectories transported from high altitudes (1500 m) were corresponding with the higher concentration at Site B, C and D from the first three days, while those from lower altitudes (< 500 m) were corresponding with the lower concentration. In other seasonal periods of transition, autumn and winter, the trajectories seemingly have no effect on the concentration variation. Thus, the transboundary transportation of the air parcels would not be a definite parameter for controlling the concentration of NH_3(g).

References

Carslaw D.C. (2019). The openair manual — open-source tools for analysing airpollution data. Manual for version2.6-6. *University of York. November*.

Donnelly, A., Misstear, B., Broderick, B. (2011). Application of nonparametric regression methods to study the relationship between NO_2 concentrations and local wind direction and speed at background sites. *Science of the Total Environment* **409(6)**: 1134-1144. https://doi.org/10.1016/j.scitotenv.2010.12.001.

Henry, R., Norris, G. A., Vedantham, R., Turner, J. R. (2009). Source region identification using kernel smoothing. *Environmental Science and Technology* **43(11)**: 4090-4097. https://doi.org/10.1021/es8011723.

Nair, A. A., Yu, F. (2020). Quantification of atmospheric ammonia concentrations: A review of its measurement and modeling. *Atmosphere* **11(10)**: 1-35. https://doi.org/10.3390/atmos11101092.

Pancras, J. P., Vedantham, R., Landis, M. S., Norris, G. A., Ondov, J. M. (2011). Application of EPA unmix and nonparametric wind regression on high time resolution trace elements and speciated mercury in Tampa, Florida Aerosol. *Environmental Science and Technology* **45(8)**: 3511-3518. https://doi.org/10.1021/es103400h.

Zhu, L., Henze, D. K., Bash, J. O., Cady-Pereira, K. E., Shephard, M. W., Luo, M., Capps, S. L. (2015). Sources and Impacts of Atmospheric NH_3: Current Understanding and Frontiers for Modeling, Measurements, and Remote Sensing in North America. *Current Pollution Reports* **1(2):** 95–116. https://doi.org/10.1007/s40726-015-0010-4.

Appendix

I. Kobe sample

Atmospheric concentration (ppb)									
Date	Site A	Site B	Site C	Site D	Site E	Site F	Site G	Site H	Site I
20080902	1.28	2.80	2.20	2.11	2.41	3.46	2.62	2.96	4.25
20080916	1.88	3.63	2.15	2.74	2.40	3.44	2.48	3.69	2.88
20080930	0.72	2.46	1.98	1.89	1.64	3.26	1.85	1.59	2.57
20081014	0.79	1.88	1.48	1.27	1.14	2.84	0.93	0.52	1.60
20081028	0.20	1.47	1.35	1.24	1.74	2.22	2.03	1.61	2.66
20081111	0.72	2.45	2.40	2.08	2.89	3.67	2.66	1.78	3.19
20081125	0.71	2.68	2.23	1.80	2.36	2.45	2.27	1.30	2.96
20081209	0.56	2.43	2.67	2.01	2.93	2.94	2.34	1.52	2.91
20081223	0.96	3.39	3.26	2.96	3.25	3.13	3.29	2.16	4.65
20090106	0.26	1.25	1.26	1.60	1.46	3.44	2.63	1.35	2.26
20090120	0.29	1.18	0.98	1.97	2.52	3.04	2.79	1.50	2.64
20090203	0.35	1.92	1.12	2.67	3.55	4.45	4.10	1.71	4.36
20090217	0.20	1.01	1.31	1.41	1.95	3.87	2.64	1.37	1.97
20090303	0.39	1.37	1.51	1.48	2.74	3.04	2.06	1.95	2.53
20090317	0.30	0.96	1.02	2.28	2.07	4.26	2.22	1.92	1.83
20090331	0.26	1.05	1.22	1.71	1.97	2.54	1.58	1.52	2.20
20090414	1.36	2.44	1.94	2.28	2.42	3.88	2.49	1.84	2.32
20090428	1.22	1.99	1.46	1.84	1.69	2.36	1.50	1.58	2.82
20090512	0.00	3.98	3.06	2.78	3.08	4.22	2.51	2.00	2.95
20090526	0.84	2.16	0.97	1.35	1.17	1.22	0.90	1.02	1.46
20090609	1.06	1.76	1.21	1.66	1.76	3.18	1.61	1.67	2.39
20090623	0.90	1.85	1.42	1.74	1.75	1.86	1.37	0.75	1.88
20090707	1.97	1.68	1.48	1.84	1.62	2.34	1.55	1.66	2.58
20090721	2.57	2.40	1.89	2.12	2.93	3.01	1.75	2.44	2.68
20090804	2.08	2.53	1.84	1.76	1.92	3.32	2.65	2.34	2.64
20090818	1.82	2.47	2.13	2.15	2.50	3.11	2.02	1.94	2.93

II. Kitakyushu sample (Tobata)

	Date	Sample	IC result (mg/l)	Atm. conc. (ppb)
March – 201803	180312	P-NH3-Tobata-01	0.119	2.8
	180319	P-NH3-Tobata-02	0.001	-2.3(*)
	180326	P-NH3-Tobata-03	0.114	2.6
April – 201804	180402	P-NH3-Tobata-04	0.190	6.4
	180409	P-NH3-Tobata-05	0.110	2.9
	180416	P-NH3-Tobata-06	0.122	3.4
	180423	P-NH3-Tobata-07	0.154	4.8
May – 201805	180501	P-NH3-Tobata-08	0.150	5.1
	180507	P-NH3-Tobata-09	0.135	6.0
	180514	P-NH3-Tobata-10	0.177	7.0
	180521	P-NH3-Tobata-11	0.088	3.1
	180528	P-NH3-Tobata-12	0.139	5.3
June – 201806	180604	P-NH3-Tobata-13	0.223	8.9
	180611	P-NH3-Tobata-14	0.116	4.3
	180618	P-NH3-Tobata-15	0.132	5.0
	180625	P-NH3-Tobata-16	0.113	4.1
July – 201807	180702	P-NH3-Tobata-17	0.079	3.0
	180709	P-NH3-Tobata-18	0.132	5.3
	180717	P-NH3-Tobata-19	0.189	6.8
	180723	P-NH3-Tobata-20	0.085	3.8
	180730	P-NH3-Tobata-21	0.121	4.9
August – 201808	180806	P-NH3-Tobata-22	0.108	4.2
	180813	P-NH3-Tobata-23	0.109	4.3
	180820	P-NH3-Tobata-24	0.084	3.2
	180827	P-NH3-Tobata-25	0.059	2.1
September – 201809	180903	P-NH3-Tobata-26	0.085	3.4
	180911	P-NH3-Tobata-27	0.100	3.5
	180918	P-NH3-Tobata-28	0.075	3.0
	180925	P-NH3-Tobata-29	0.096	3.9

October – 201810	181001	P-NH3-Tobata-30	0.070	2.9
	181009	P-NH3-Tobata-31	0.124	4.2
	181015	P-NH3-Tobata-32	0.139	5.5
	181022	P-NH3-Tobata-33	0.091	3.4
	181029	P-NH3-Tobata-34	0.093	3.5
November – 201811	181105	P-NH3-Tobata-35	0.130	5.4
	181105	P-NH3-Tobata-36	0.119	4.9
	181112	P-NH3-Tobata-37	0.114	4.7
	181119	P-NH3-Tobata-38	0.104	4.3
	181126	P-NH3-Tobata-39	0.112	4.7
December –201812	181203	P-NH3-Tobata-40	0.164	6.9
	181210	P-NH3-Tobata-41	0.092	3.8
	181217	P-NH3-Tobata-42	0.109	4.5
	181225	P-NH3-Tobata-43	0.142	5.2
January – 201901	190107	P-NH3-Tobata-44	0.158	3.4
	190115	P-NH3-Tobata-45	0.127	4.4
	190121	P-NH3-Tobata-46	0.099	4.4
	190128	P-NH3-Tobata-47	0.099	3.8
February – 201902	190204	P-NH3-Tobata-48	0.063	2.7
	190212	P-NH3-Tobata-49	0.076	2.8
	190218	P-NH3-Tobata-50	0.024	1.1
Note: (*) shows the minus value, which was replaced by zero in the calculation of monthly mean concentration.				

	Blank	IC results (mg/l)
March – 201803	P-NH3-Tobata-BLK1803	0.054
April – 201804	P-NH3-Tobata-BLK1804	0.043
May – 201805	P-NH3-Tobata-BLK1805	0.016
June – 201806	P-NH3-Tobata-BLK1806	0.017
July – 201807	P-NH3-Tobata-BLK1807	0.010
August – 201808	P-NH3-Tobata-BLK1808	0.011
September – 201809	P-NH3-Tobata-BLK1809	0.007
October – 201810	P-NH3-Tobata-BLK1810	0.012
November – 201811	P-NH3-Tobata-BLK1811	0.005
December – 201812	P-NH3-Tobata-BLK1812	0.005
January – 201901	P-NH3-Tobata-BLK1901	0.012
February – 201902	P-NH3-Tobata-BLK1902	0.002

III. Hanoi Daily sample

		Date	Sample	IC results (mg/l)	Atm. Conc. (ppb)
Spring	Site A	180305	P-NH3-Hanoi-01	0.116	2.8
		180306	P-NH3-Hanoi-02	0.107	48.2
		180307	P-NH3-Hanoi-03	0.094	40.5
		180308	P-NH3-Hanoi-04	0.072	26.6
		180309	P-NH3-Hanoi-05	0.085	34.8
		180310	P-NH3-Hanoi-06	0.089	37.1
		180311	P-NH3-Hanoi-07	0.101	44.4
	Site B	180305	P-NH3-Hanoi-15	0.184	85.9
		180306	P-NH3-Hanoi-16	0.169	76.3
		180307	P-NH3-Hanoi-17	0.121	47.2
		180308	P-NH3-Hanoi-18	0.094	30.7
		180309	P-NH3-Hanoi-19	0.170	77.0
		180310	P-NH3-Hanoi-20	0.148	64.0
		180311	P-NH3-Hanoi-21	0.203	97.4
	Site C	180305	P-NH3-Hanoi-08	0.123	52.8
		180306	P-NH3-Hanoi-09	0.126	54.7
		180307	P-NH3-Hanoi-10	0.095	35.9
		180308	P-NH3-Hanoi-11	0.067	18.8
		180309	P-NH3-Hanoi-12	0.101	39.3
		180310	P-NH3-Hanoi-13	0.096	36.2
		180311	P-NH3-Hanoi-14	0.138	61.9
	Site D	180305	P-NH3-Hanoi-22	0.181	86.3
		180306	P-NH3-Hanoi-23	0.190	92.0
		180307	P-NH3-Hanoi-24	0.115	46.7
		180308	P-NH3-Hanoi-25	0.081	25.4
		180309	P-NH3-Hanoi-26	0.133	57.4
		180310	P-NH3-Hanoi-27	0.137	59.8
		180311	P-NH3-Hanoi-28	0.176	83.5

		Date	Sample	IC results (mg/l)	Atm. Conc. (ppb)
Summer	Site A	180702	P-NH3-Hanoi-01	0.118	41.6
		180703	P-NH3-Hanoi-02	0.104	32.7
		180704	P-NH3-Hanoi-03	0.147	59.3
		180705	P-NH3-Hanoi-04	0.152	62.3
		180706	P-NH3-Hanoi-05	0.161	67.4
		180707	P-NH3-Hanoi-06	0.161	67.8
		180708	P-NH3-Hanoi-07	0.156	64.8
	Site B	180702	P-NH3-Hanoi-15	0.486	268.2
		180703	P-NH3-Hanoi-16	0.521	289.5
		180704	P-NH3-Hanoi-17	0.488	269.9
		180705	P-NH3-Hanoi-18	0.237	116.7
		180706	P-NH3-Hanoi-19	0.231	113.3
		180707	P-NH3-Hanoi-20	0.152	65.0
		180708	P-NH3-Hanoi-21	0.159	69.8
	Site C	180702	P-NH3-Hanoi-08	0.262	90.5
		180703	P-NH3-Hanoi-09	0.186	44.0
		180704	P-NH3-Hanoi-10	0.202	54.1
		180705	P-NH3-Hanoi-11	0.187	44.9
		180706	P-NH3-Hanoi-12	0.210	58.5
		180707	P-NH3-Hanoi-13	0.199	52.2
		180708	P-NH3-Hanoi-14	0.195	49.6
	Site D	180702	P-NH3-Hanoi-22	0.378	180.0
		180703	P-NH3-Hanoi-23	0.249	101.9
		180704	P-NH3-Hanoi-24	0.244	99.0
		180705	P-NH3-Hanoi-25	0.165	50.8
		180706	P-NH3-Hanoi-26	0.153	43.6
		180707	P-NH3-Hanoi-27	0.154	43.7
		180708	P-NH3-Hanoi-28	0.162	48.6

		Date	Sample	IC results (mg/l)	Atm. Conc. (ppb)
Transition	Site A	181002	P-NH3-Hanoi-01	0.043	24.8
		181003	P-NH3-Hanoi-02	0.058	33.9
		181004	P-NH3-Hanoi-03	0.046	26.8
		181005	P-NH3-Hanoi-04	0.061	35.5
		181006	P-NH3-Hanoi-05	0.051	29.8
		181007	P-NH3-Hanoi-06	0.077	45.5
		181008	P-NH3-Hanoi-07	0.011	5.1
	Site B	181002	P-NH3-Hanoi-15	0.117	69.5
		181003	P-NH3-Hanoi-16	0.152	90.4
		181004	P-NH3-Hanoi-17	0.138	82.1
		181005	P-NH3-Hanoi-18	0.144	85.8
		181006	P-NH3-Hanoi-19	0.101	59.9
		181007	P-NH3-Hanoi-20	0.218	130.6
		181008	P-NH3-Hanoi-21	0.017	8.4
	Site C	181002	P-NH3-Hanoi-08	0.057	32.8
		181003	P-NH3-Hanoi-09	0.069	39.9
		181004	P-NH3-Hanoi-10	0.035	19.1
		181005	P-NH3-Hanoi-11	0.095	55.7
		181006	P-NH3-Hanoi-12	0.076	44.5
		181007	P-NH3-Hanoi-13	0.128	75.8
		181008	P-NH3-Hanoi-14	0.022	11.6
	Site D	181015	P-NH3-Hanoi-22	0.023	9.9
		181016	P-NH3-Hanoi-23	0.013	4.0
		181017	P-NH3-Hanoi-24	0.009	1.6
		181018	P-NH3-Hanoi-25	0.008	1.1
		181019	P-NH3-Hanoi-26	0.011	2.7
		181020	P-NH3-Hanoi-27	0.043	22.2
		181021	P-NH3-Hanoi-28	0.047	24.5

		Date	Sample	IC results (mg/l)	Atm. Conc. (ppb)
Autumn	Site A	181113	P-NH3-Hanoi-01	0.018	10.5
		181114	P-NH3-Hanoi-02	0.021	12.3
		181115	P-NH3-Hanoi-03	0.016	9.4
		181116	P-NH3-Hanoi-04	0.017	9.9
		181117	P-NH3-Hanoi-05	0.017	10.3
		181118	P-NH3-Hanoi-06	0.030	17.8
		181119	P-NH3-Hanoi-07	0.019	11.2
	Site B	181113	P-NH3-Hanoi-15	n.a.	n.a.
		181114	P-NH3-Hanoi-16	0.065	39.8
		181115	P-NH3-Hanoi-17	0.074	44.9
		181116	P-NH3-Hanoi-18	0.047	28.8
		181117	P-NH3-Hanoi-19	0.076	46.4
		181118	P-NH3-Hanoi-20	0.033	20.1
		181119	P-NH3-Hanoi-21	0.031	19.0
	Site C	181113	P-NH3-Hanoi-08	0.032	19.3
		181114	P-NH3-Hanoi-09	0.018	11.2
		181115	P-NH3-Hanoi-10	0.027	16.7
		181116	P-NH3-Hanoi-11	0.030	18.4
		181117	P-NH3-Hanoi-12	0.017	10.6
		181118	P-NH3-Hanoi-13	0.022	13.4
		181119	P-NH3-Hanoi-14	0.018	11.1
	Site D	181113	P-NH3-Hanoi-22	0.048	28.9
		181114	P-NH3-Hanoi-23	0.018	10.8
		181115	P-NH3-Hanoi-24	0.014	8.6
		181116	P-NH3-Hanoi-25	0.017	10.1
		181117	P-NH3-Hanoi-26	0.022	13.6
		181118	P-NH3-Hanoi-27	0.005	2.9
		181119	P-NH3-Hanoi-28	0.003	1.5

		Date	Sample	IC results (mg/l)	Atm. Conc. (ppb)
Winter	Site A	190114	P-NH3-Hanoi-01	0.221	50.7
		190115	P-NH3-Hanoi-02	0.065	31.2
		190116	P-NH3-Hanoi-03	0.041	16.8
		190117	P-NH3-Hanoi-04	0.071	35.2
		190118	P-NH3-Hanoi-05	0.133	72.5
		190119	P-NH3-Hanoi-06	0.132	72.0
		190120	P-NH3-Hanoi-07	0.133	72.7
	Site B	190114	P-NH3-Hanoi-15	n.a.	n.a.
		190115	P-NH3-Hanoi-16	0.088	45.7
		190116	P-NH3-Hanoi-17	0.054	25.4
		190117	P-NH3-Hanoi-18	0.078	39.7
		190118	P-NH3-Hanoi-19	0.114	61.5
		190119	P-NH3-Hanoi-20	0.189	107.2
		190120	P-NH3-Hanoi-21	0.156	87.0
	Site C	190114	P-NH3-Hanoi-08	0.077	44.0
		190115	P-NH3-Hanoi-09	0.061	34.6
		190116	P-NH3-Hanoi-10	0.082	47.2
		190117	P-NH3-Hanoi-11	0.061	34.7
		190118	P-NH3-Hanoi-12	0.075	43.0
		190119	P-NH3-Hanoi-13	0.130	76.3
		190120	P-NH3-Hanoi-14	0.075	42.9
	Site D	190114	P-NH3-Hanoi-22	0.068	36.0
		190115	P-NH3-Hanoi-23	0.026	10.4
		190116	P-NH3-Hanoi-24	0.014	3.0
		190117	P-NH3-Hanoi-25	0.033	14.4
		190118	P-NH3-Hanoi-26	0.038	17.2
		190119	P-NH3-Hanoi-27	0.073	38.7
		190120	P-NH3-Hanoi-28	0.041	19.3
Note: n.a. shows the samples affected by human-induce errors.					

Blank values of daily samples (mg/l)					
	Spring	Summer	Transition	Autumn	Winter
Site A	0.0279	0.0500	0.0023	0.0004	0.0124
Site B	0.0431	0.0447	0.0029	N.D.	0.0126
Site C	0.0363	0.1135	0.0034	N.D.	0.0045
Site D	0.0387	0.1828	0.0063	N.D.	0.0093
Note: N.D. shows not detected value by Ion Chromatography analysis.					

IV. Hanoi Weekly sample

	Date	Sample	IC results (mg/l)	Atm. conc. (ppb)
March – 201803	180312	P-NH3-Hanoi-30	0.49	27.5
	180319	P-NH3-Hanoi-31	0.597	36.6
	180326	P-NH3-Hanoi-32	0.516	29.6
	180402	P-NH3-Hanoi-33	0.51	28.8
April – 201804	180409	P-NH3-Hanoi-35	0.46	14.7
	180416	P-NH3-Hanoi-36	0.442	13.1
	180423	P-NH3-Hanoi-37	0.421	11.2
	180502	P-NH3-Hanoi-38	0.494	13.5
May – 201805	180507	P-NH3-Hanoi-40	0.431	30.7
	180514	P-NH3-Hanoi-41	0.52	29.1
	180521	P-NH3-Hanoi-42	0.428	21.4
	180528	P-NH3-Hanoi-43	0.455	23.6
June – 201806	180604	P-NH3-Hanoi-44	0.47	25.1
	180611	P-NH3-Hanoi-30	0.46	21.0
	180618	P-NH3-Hanoi-31	0.516	25.6
	180625	P-NH3-Hanoi-32	0.437	18.9
July – 201807	180702	P-NH3-Hanoi-33	0.513	25.2
	180709	P-NH3-Hanoi-35	0.688	47.1
	180716	P-NH3-Hanoi-36	0.667	46.5
	180723	P-NH3-Hanoi-37	0.528	35.3
	180730	P-NH3-Hanoi-38	1.025(*)	30.8
August – 201808	180806	P-NH3-Hanoi-39	0.586	40.1
	180813	P-NH3-Hanoi-30	0.469	31.7
	180904	P-NH3-Hanoi-31	0.303	21.7
September – 201809	180910	P-NH3-Hanoi-40	0.695	43.6
	180917	P-NH3-Hanoi-41	0.74	41.0
	180924	P-NH3-Hanoi-42	0.622	31.5
	181001	P-NH3-Hanoi-43	0.628	32.2
October – 201810	181008	P-NH3-Hanoi-29	0.627	37.2
	181015	P-NH3-Hanoi-30	0.468	35.0
	181024	P-NH3-Hanoi-31	0.592	35.6
	181029	P-NH3-Hanoi-33	0.346	34.5
November – 201811	181105	P-NH3-Hanoi-34	0.418	31.0
	181112	P-NH3-Hanoi-35	0.553	41.7
	181119	P-NH3-Hanoi-36	0.545	40.6
	181126	P-NH3-Hanoi-37	0.53	40.4
	181203	P-NH3-Hanoi-38	0.52	39.2

December – 201812	181210	P-NH3-Hanoi-51	1.347(*)	37.5
	181217	P-NH3-Hanoi-31	0.362	6.6
	181224	P-NH3-Hanoi-32	0.676	33.3
	181231	P-NH3-Hanoi-33	1.773(*)	37.5
January – 201901	190107	P-NH3-Hanoi-34	0.438	13.3
	190114	P-NH3-Hanoi-40	0.825	47.7
	190121	P-NH3-Hanoi-41	0.719	38.5
	190201	P-NH3-Hanoi-42	2.27(*)	37.5
February – 201902	190212	P-NH3-Hanoi-43	1.047	41.4
	190218	P-NH3-Hanoi-44	0.987	59.8
	190225	P-NH3-Hanoi-31	0.895	43.7
	190403	P-NH3-Hanoi-32	1.004	52.9
Note: (*) show the abnormally high values due to human-induced errors, the corresponding atm. conc. were replaced by the mean of the corresponding season.				

	Blank code	IC results (mg/l)
March – 201803	P-NH3-Hanoi-34BLK	0.170
April – 201804	P-NH3-Hanoi-39BLK	0.288
May – 201805	P-NH3-Hanoi-45BLK	0.166
June – 201806	P-NH3-Hanoi-34BLK	0.205
July – 201807	P-NH3-Hanoi-51BLK	0.101
August – 201808	P-NH3-Hanoi-34BLK	0.082
September – 201809	P-NH3-Hanoi-44BLK	0.240
October – 201810	P-NH3-Hanoi-50BLK	0.052
November – 201811	P-NH3-Hanoi-39BLK	0.059
December – 201812	P-NH3-Hanoi-30BLK	0.288
January – 201901	P-NH3-Hanoi-45BLK	0.283
February – 201902	P-NH3-Hanoi-33BLK	0.408